Pregnancy-specific responses to COVID-19 are revealed by high-throughput proteomics of human plasma

Nardhy Gomez-Lopez (ngomezlo@med.wayne.edu)
Wayne State University School of Medicine

Roberto Romero
https://orcid.org/0000-0002-4448-5121

Maria Escobar
Fundacion Valle del Lili

Javier Carvajal
Fundacion Valle del Lili

Maria Echavarria
Fundacion Valle del Lili

Ludwig Albornoz
Fundacion Valle del Lili

Daniela Nasner
Fundacion Valle del Lili

Derek Miller
Wayne State University https://orcid.org/0000-0002-5812-7771

Dahiana Gallo
Wayne State University School of Medicine

Jose Galaz
Wayne State University School of Medicine https://orcid.org/0000-0002-8160-8581

Marcia Arenas-Hernandez
Wayne State University School of Medicine https://orcid.org/0000-0002-1178-6112

Gaurav Bhatti
Perinatology Research Branch

Bogdan Done
Wayne State University School of Medicine https://orcid.org/0000-0002-7977-3764

Maria Zambrano
Fundacion Valle del Lili

Isabella Ramos
Fundacion Valle del Lili

Paula Fernandez

Fundacion Valle del Lili
Leandro Posada
Fundacion Valle del Lili
Tinnakorn Chaiworapongsa
Wayne State University
Eunjung Jung
Wayne State University School of Medicine
Valeria Garcia-Flores
Wayne State University School of Medicine
Manaphat Suksai
Wayne State University School of Medicine https://orcid.org/0000-0003-4441-4988
Francesca Gotsch
Wayne State University School of Medicine
Mariachiara Bosco
Wayne State University School of Medicine
Nandor Than
Research Centre for Natural Sciences
Adi Tarca
Wayne State University School of Medicine https://orcid.org/0000-0003-1712-7588

Article

Keywords: angiogenesis, circulation, cytokine storm, maternal immune activation, proteome, SARS-CoV-2

Posted Date: August 22nd, 2022

DOI: https://doi.org/10.21203/rs.3.rs-1906806/v1

Pregnancy-specific responses to COVID-19 are revealed by high-throughput proteomics of human plasma

Nardhy Gomez-Lopez[1,2,3,*], Roberto Romero[1,3-7,*], María Fernanda Escobar[8,9], Javier Andres Carvajal[8,9], Maria Paula Echavarria[8,9], Ludwig L. Albornoz[10,11], Daniela Nasner[12], Derek Miller[1,2], Dahiana M. Gallo[1,2], Jose Galaz[1,2,13], Marcia Arenas-Hernandez[1,2], Gaurav Bhatti[1,2], Bogdan Done[1,2], Maria Andrea Zambrano[9], Isabella Ramos[9], Paula Andrea Fernandez[9], Leandro Posada[9], Tinnakorn Chaiworapongsa[1,2], Eunjung Jung[1,2], Valeria Garcia-Flores[1,2], Manaphat Suksai[1,2], Francesca Gotsch[1,2], Mariachiara Bosco[1,2], Nandor Gabor Than[14-16], Adi L. Tarca[1,2,17,*]

[1]Perinatology Research Branch, Division of Obstetrics and Maternal-Fetal Medicine, Division of Intramural Research, *Eunice Kennedy Shriver* National Institute of Child Health and Human Development, National Institutes of Health, U.S. Department of Health and Human Services (NICHD/NIH/DHHS); Bethesda, Maryland, and Detroit, Michigan, USA;

[2]Department of Obstetrics and Gynecology, Wayne State University School of Medicine, Detroit, Michigan, USA;

[3]Department of Biochemistry, Microbiology and Immunology, Wayne State University School of Medicine, Detroit, Michigan, USA;

[4]Department of Obstetrics and Gynecology, University of Michigan, Ann Arbor, Michigan, USA;

[5]Department of Epidemiology and Biostatistics, Michigan State University, East Lansing, Michigan, USA;

[6]Center for Molecular Medicine and Genetics, Wayne State University, Detroit, Michigan, USA;

[7]Detroit Medical Center, Detroit, Michigan, USA;

[8]Department of Obstetrics and Gynecology, Fundacion Valle del Lili, Cali, Colombia

[9]Department of Obstetrics and Gynecology, School of Medicine, Universidad Icesi, Cali, Colombia

[10]Department of Pathology and Laboratory Medicine, Fundación Valle del Lili, Cali, Colombia.

[11]Facultad de Ciencias de la Salud, Universidad Icesi, Cali, Colombia

[12]Centro de Investigaciones Clínicas, Fundación Valle del Lili, Cali, Colombia

[13]Division of Obstetrics and Gynecology, School of Medicine, Faculty of Medicine, Pontificia Universidad Católica de Chile, Santiago, Chile

[14]Systems Biology of Reproduction Research Group, Institute of Enzymology, Research Centre for Natural Sciences, Budapest, Hungary

[15]Maternity Private Clinic of Obstetrics and Gynecology, Budapest, Hungary

[16]First Department of Pathology and Experimental Cancer Research, Semmelweis University, Budapest, Hungary

[17]Department of Computer Science, Wayne State University College of Engineering, Detroit, Michigan, USA

*Corresponding authors:

ngomezlo@med.wayne.edu

prbchiefstaff@med.wayne.edu

atarca@med.wayne.edu

ABSTRACT

Pregnant women are at greater risk of adverse outcomes, including mortality, as well as obstetrical complications resulting from COVID-19. However, pregnancy-specific changes that underlie such worsened outcomes remain unclear. Herein, we profiled the plasma proteome of pregnant and non-pregnant COVID-19 patients and controls and showed alterations that display a dose-response relationship with disease severity; yet, such proteomic perturbations are dampened during pregnancy. In both pregnant and non-pregnant state, the proteome response induced by COVID-19 showed enrichment of mediators implicated in cytokine storm, endothelial dysfunction, and angiogenesis. Shared and pregnancy-specific proteomic changes were identified: pregnant women display a tailored response that may protect the conceptus from heightened inflammation, while non-pregnant individuals display a stronger response to repel infection. Furthermore, the plasma proteome can accurately identify COVID-19 patients, even when asymptomatic or with mild symptoms. This study represents the most comprehensive characterization of the plasma proteome of pregnant and non-pregnant COVID-19 patients.

KEYWORDS: angiogenesis, circulation, cytokine storm, maternal immune activation, proteome, SARS-CoV-2

INTRODUCTION

Coronavirus disease 2019 (COVID-19) represents an ongoing threat to people around the world[1,2]. To date, over 400 million people have been infected with SARS-CoV-2, the virus responsible for COVID-19[3], and the death toll has neared 6 million[1]. A growing body of evidence has indicated that pregnant women are at an increased risk of adverse outcomes resulting from COVID-19, ranging from greater rates of admission to the intensive care unit and need for mechanical ventilation to higher risk of death compared to non-pregnant women[4-6]. Moreover, pregnant women with COVID-19 have also been shown to experience more obstetrical complications such as preeclampsia[7,8], preterm birth[7,8], and stillbirth[9]. Thus, COVID-19 during pregnancy not only adversely affects the mother, but can also negatively affect quality of life for the offspring[10-18]. Hence, there is an urgent need to understand the pregnancy-driven biological pathways, including immune responses, underlying the increased susceptibility to severe COVID-19 and obstetrical disease.

Upon the onset of the COVID-19 pandemic, multiple investigations have sought to uncover the effects of SARS-CoV-2 infection on maternal, fetal/placental, and neonatal immunity[19-32]. Indeed, we and others have characterized the changes in systemic parameters such as cellular immune responses, virus-specific immunoglobulins, and inflammatory mediators in the maternal peripheral blood and/or cord blood to generate a profile of the maternal-fetal immune responses against SARS-CoV-2 infection[26,33-36]. In particular, comparative studies of pregnant and non-pregnant COVID-19 patients have indicated specific alterations in systemic cytokine levels, peripheral leukocyte subsets, and their activation status[37-40], providing insights into the mechanisms underlying the increased susceptibility to severe COVID-19 during pregnancy. Such findings are consistent with longitudinal analyses of the general population

showing that dynamic changes in systemic cytokines[41,42], bulk or single-cell gene expression[43], and leukocyte subsets[43,44] are characteristic of severe COVID-19. The integration of such omics datasets has also revealed the enrichment of specific cellular processes contributing to disease status and severity, such as inflammation, cell cycle and death, and metabolism[45]. Thus, to further understand the consequences of COVID-19 in pregnant women, the application of high-throughput omics platforms has facilitated the identification of relevant molecules and biological pathways implicated in this disease. Indeed, a recent study profiled over 1,400 proteins in maternal peripheral blood and cord blood and indicated that pregnant women with severe COVID-19 display increased inflammatory and anti-viral signaling compared to asymptomatic pregnant women, while their offspring displayed elevated cytokines associated with T-cell responses and/or inflammasome activation[46]. However, the proteomic dysregulation that distinguishes pregnant from non-pregnant COVID-19 patients has not been elucidated.

Aptamer-based technologies that allow the identification and monitoring of over 1,000 potential target proteins have been utilized to profile the human proteome during normal pregnancy and/or its complications in the maternal plasma[47-51] and amniotic fluid[52]. Yet, the much-expanded version (4.1) of the SOMAScan platform, which allows measuring of over 7,000 analytes, had not been utilized to study pathology in obstetrics. In this study, we classified pregnant and non-pregnant women according to COVID-19 status and severity, and performed proteomic profiling using the high-throughput SOMAScan platform to determine the differentially affected proteins. Furthermore, we utilized computational approaches to compare and contrast the specific proteins and signaling pathways implicated in COVID-19 between the pregnant and non-pregnant states to enable the development and implementation of predictive models of disease.

RESULTS

Characteristics of the study population

Pregnant individuals: Plasma samples were collected from 101 pregnant women (23.2 – 39.3 weeks of gestation), including those diagnosed with COVID-19 at the time of admission (n = 72) and those who tested negative for SARS-CoV-2 during prenatal care visits (hereafter referred to as pregnant controls; n = 29) (Fig. 1a&b and Table 1). Parameters such as maternal age, BMI, parity, and frequency of chronic hypertension and diagnosis of preeclampsia in the current pregnancy were comparable between the pregnant COVID-19 and control groups (Table 1). Gestational age at delivery was similar between groups; yet, sampling of COVID-19 cases was performed about 5 weeks earlier in gestation than in controls [median weeks (IQR) controls: 36.1 (32.6-37.5) vs. COVID-19: 31.3 (28.1-35.6), $p < 0.05$] (Table 1), which was considered in the data analysis. Among the pregnant COVID-19 cases, 6 (8%) were asymptomatic, 20 (28%) were mild, 13 (18%) were moderate, 12 (17%) were severe, and 21 (29%) were critically ill according to NIH classification[53].

Non-pregnant individuals: Plasma samples were also collected from 93 non-pregnant individuals, which included 52 COVID-19 cases and 41 controls (Fig. 1a and Table 1). Among the non-pregnant COVID-19 cases, 1 (2%) was mild, 4 (8%) were moderate, 12 (23%) were severe, and 35 (67%) were critically ill.

COVID-19 drives shared and unique changes in the plasma proteome in pregnant and non-pregnant individuals that follow a dose response with disease severity

Over 7,000 protein analytes were determined using the SOMAScan v4.1 platform in cases and controls to characterize the plasma proteome responses induced by COVID-19

according to its severity in pregnant and non-pregnant individuals (Fig. 1a). Uniform Manifold Approximation and Projection (UMAP) plots of the proteomic profiles illustrate that patients are clustered according to COVID-19 status and severity in both pregnant (Fig. 1c) and non-pregnant (Supplementary Fig. 1) individuals. It is worth mentioning that, in non-pregnant individuals, the plasma proteome was heavily modulated by COVID-19 status, regardless of sex (Supplementary Fig. 2). Similar to the UMAP depiction, Fig. 1d&e represent an unsupervised projection of high-dimensional proteomic profiles of all controls and COVID-19 patients onto the first three principal components (PC), which can be understood as meta-proteins that are uncorrelated with each other. Notably, pregnancy status represented a source of variability in the proteome, as PC2 values (18% of variance explained) perfectly discriminated between pregnant and non-pregnant individuals ($p < 0.001$, Fig. 1d). Yet, the host response to COVID-19 represented the primary source of variability in the proteome, as PC1 and PC3 (PC1, 27% of variance explained; PC3, 6% of variance explained) were significantly different between COVID-19 cases and controls, regardless of pregnancy status ($p < 0.001$ for both, Fig. 1e). The proteomic changes with COVID-19 were larger for non-pregnant than for pregnant women based on both PC1 and PC3 (interaction $p < 0.005$) (Fig. 1e), which is partly explained by the greater proportions of severe and critically ill cases in the non-pregnant than in the pregnant population. Moreover, we observed a dose-response relationship between PC3 and disease severity, regardless of pregnancy status ($p < 0.001$ for both linear and quadratic trends, Fig. 1f). Together, these data provide an overview of the plasma proteome in pregnant and non-pregnant individuals infected with SARS-CoV-2, and suggest dramatic changes with infection in a dose-response relationship with disease severity. In addition, these data hint that the host response to SARS-CoV-2 includes

shared and unique processes between pregnant and non-pregnant individuals, which we further explore below.

The plasma proteome response to COVID-19 follows a dose-response relationship with disease severity in pregnant and non-pregnant individuals, yet such a response is dampened in pregnancy

Pregnant women have been reported to display heightened susceptibility to severe COVID-19[4-6]. Therefore, we first explored the differential effects of COVID-19 on the maternal proteome compared to control pregnancies according to disease severity (Fig. 2a). When comparing pregnant COVID-19 cases to controls after adjustment for maternal age, BMI, and gestational age at sampling, we identified 68, 81, 242, 144, and 1072 differentially abundant proteins in asymptomatic, mild, moderate, severe, and critically ill cases, respectively (Fig. 2b-f). Given that both disease severity and sample size may affect the number of differentially abundant proteins in specific groups, we next used the protein changes between critically ill patients and controls (1072 proteins) as a reference to compare with the changes observed in the less severe COVID-19 groups (Fig. 2g). The $\log_2$-transformed fold change of protein abundance between COVID-19 subgroups (i.e., asymptomatic, mild, moderate, and severe) and controls were more attenuated than those between critically ill patients and controls (regression slopes < 1.0) (Fig. 2g). Yet, the magnitude of correlation and the correlation slope followed a dose-response relationship with disease severity, and even asymptomatic patients showed plasma proteomic changes that were significantly correlated to those observed in critically ill patients ($r = 0.34$ for Asymptomatic vs. Control; $r = 0.72$ for Mild vs. Control; $r = 0.87$ for Moderate vs. Control; $r = 0.88$ for Severe vs. Control; $p < 0.001$ for all) (Fig. 2g).

We then performed the same analysis of differential protein abundance in non-pregnant patients (Fig. 3a), and identified 21, 1961, and 2966 differentially abundant proteins in moderate, severe and critically ill cases, respectively (Fig. 3b-d), after adjusting for relevant covariates. Similar to the analysis in pregnant women, the $\log_2$-transformed fold changes of protein abundance between COVID-19 subgroups and controls were more attenuated than those found between critically ill cases and controls, and followed a dose response with disease severity ($r = 0.84$ for Moderate vs. Controls; $r = 0.94$ for Severe vs. Controls; $p < 0.001$ for both) (Fig. 3e).

To contrast the magnitude of COVID-19-driven changes in the proteome between pregnant and non-pregnant patients, we then performed correlation analysis based on a core set of 486 proteins with significant and consistent changes in both pregnant and non-pregnant patients (see more details below) (Fig. 4a). By comparing the magnitude of changes between the pregnant and non-pregnant groups, we showed that the magnitude of changes for this set of core proteins were diminished during pregnancy for the same disease severity group, as indicated by the regression line slopes below 1.0 (Fig. 4b-d, $p < 0.05$ for all).

Together, these results demonstrate that there is perturbation of the plasma proteome in both pregnant and non-pregnant women with COVID-19, and that the magnitude of such changes increases with COVID-19 severity. However, relative to the plasma proteome perturbations observed in non-pregnant individuals, the magnitude of changes with COVID-19 in the pregnant state are attenuated, suggesting a dampened response.

Shared and distinct changes in the plasma proteome of pregnant and non-pregnant women with COVID-19

We then sought to further unravel pregnancy-driven differences in the plasma proteomic response to COVID-19 as well as changes that are shared between pregnant and non-pregnant states. First, we identified all proteins that were differentially abundant with COVID-19, which resulted in 708 differentially abundant proteins for pregnant women (Fig. 5a and Supplementary Table 1) and 2,605 for non-pregnant individuals (Fig. 5b and Supplementary Table 2). From these two lists, we identified 486 proteins that were significantly affected by COVID-19 in both pregnant and non-pregnant groups and had similar direction of change (Supplementary Table 2).

Next, we explored the biological processes that were enriched among the entire set of differentially abundant proteins for pregnant (708 proteins) and non-pregnant (2,605 proteins) COVID-19 patients to characterize the differences in host response (Fig. 5c-f). As expected, enriched biological processes in pregnant women with COVID-19 were fewer than those in non-pregnant patients, given the dampened protein response (Fig. 5c and Supplementary Tables 3-4). Consistent with such an observation, pregnant COVID-19 patients showed enrichment of processes related to extracellular matrix, defense response, and immune response (Fig. 5d), whereas those enriched in non-pregnant individuals included protein localization and transport, peptide biosynthesis, and translation (Fig. 5e and Supplementary Tables 3-4). Shared processes were characterized by cell adhesion and immune responses as well as response to wounding and blood coagulation (Fig. 5f).

In addition to biological processes, we also evaluated the enrichment of pathways and gene sets derived from the C2 collection of the MSigDB database (Fig. 5g). Similar to biological processes, pathways enriched in pregnant women with COVID-19 included terms related to extracellular matrix; yet, pathways associated with viral infection or anti-viral defenses were also observed (Fig. 5h and Supplementary Table 5). Enriched pathways in non-pregnant COVID-19

patients included terms related to platelet activation, VEGF, and PDGF (Fig. 5i), while shared pathways included virus- and cancer-related terms (Fig. 5j and Supplementary Table 6).

Together, these data further demonstrate that, although there is a set of common responses to COVID-19 in both pregnant and non-pregnant state, pregnancy-specific changes exist: while non-pregnant women display a stronger proteomic response to fight off infection, pregnant women exhibit a tailored immune proteomic response that may protect the conceptus from unwarranted exposure to inflammation.

COVID-19 drives distinct angiogenic and inflammatory proteomic changes in pregnant and non-pregnant individuals

Given our finding that pregnancy modifies the proteomic response to COVID-19, we further investigated whether any proteins were dysregulated with COVID-19 in opposite directions between pregnant and non-pregnant patients (see Methods). This analysis identified a core set of 33 proteins with opposing direction of change (Fig. 6a) and included proteins related to angiogenesis and wound healing as well as alarmins, cytokines, and growth factors (Table 2). Proteins that decreased with COVID-19 in pregnancy but were increased in non-pregnant cases included vascular endothelial growth factor receptor 1 (VEGF-sR1 or sFLT1) and angiotensinogen (AGT); yet, this could potentially be explained by their already elevated baseline among pregnant patients (Fig. 6b&c and Table 2). Consistent with these findings, proteins that underwent pregnancy-specific regulation with COVID-19 were enriched for biological processes and pathways related to vasodilation, angiogenesis, and regulation of inflammatory response (Supplementary Table 7). A previous report indicated that COVID-19 during pregnancy is characterized by a profile of proteomic factors that is distinct from but

242 overlaps with that observed in preeclampsia[7], an obstetric syndrome characterized by
243 intravascular inflammation[54]. Therefore, we further evaluated changes in angiogenic or
244 endothelial factors between pregnant and non-pregnant COVID-19 patients. Several factors such
245 as soluble TNF receptor II (TNFRSF1B) and von Willebrand factor (VWF) were found to
246 increase with COVID-19 regardless of pregnancy status (Fig. 6d&e). Notably, neutrophil
247 elastase (ELANE), a neutrophil degranulation factor[55] as well as a component of neutrophil
248 extracellular traps (NETs)[56], was elevated in both pregnant and non-pregnant COVID-19 cases
249 (Fig. 6f), as was histone H3.1 (H3C1), another NET component (Fig. 6g). These results provide
250 insight into the unique biological processes in pregnant and non-pregnant individuals: while non-
251 pregnant individuals exhibit increased abundance of angiogenic and inflammatory proteins in the
252 circulation, the proteome of pregnant women hints at a systemic inflammatory response and no
253 increase in anti-angiogenic sFLT-1, which is already elevated in the pregnant state. The latter
254 finding suggests that COVID-19 induces a stereotypical inflammatory response in the maternal
255 circulation that shares pathways with the syndrome of preeclampsia.
256
257 **Pregnant women with COVID-19 display a dampened systemic cytokine response**
258 COVID-19 is characterized by a cytokine storm, components of which can display a
259 dose-response with disease severity[41]. Therefore, we next focused on the protein expression
260 changes of specific inflammatory mediators (Fig. 7a). The classical inflammatory cytokines IL-6,
261 IL-1β, and IL-18 were increased in COVID-19 cases compared to controls for both pregnant and
262 non-pregnant patients; yet, the latter two did not reach significance in pregnant women (IL-1β, p
263 = 0.074; IL-18, p = 0.052), likely due to the dampened proteomic response (Fig. 7b-d). Similarly,
264 TNF and IL-17A were upregulated with COVID-19 in non-pregnant patients and only showed a

slight tendency to increase during pregnancy (Fig. 7e&f). The alarmin IL-1α was found to be downregulated only in pregnant COVID-19 cases, although a tendency towards the same reduction was observed in non-pregnant patients (Fig. 7g). By contrast, IFNγ was reduced with COVID-19 in non-pregnant individuals but not pregnant patients (Fig. 7h). The anti-inflammatory cytokine IL-10 was downregulated in pregnant and non-pregnant COVID-19 cases (Fig. 7i), whereas TGFβ1 was upregulated in both groups (Fig. 7j). Several chemokines were also found to exhibit differential regulation with COVID-19 in the pregnant and non-pregnant states: CXCL10 and CCL22 were consistently increased or diminished, respectively, in both non-pregnant and pregnant cases; yet, CCL1 was reduced and CXCL13 was increased only in non-pregnant COVID-19 patients, although data from pregnant patients showed similar tendencies (Fig. 7k-n). These findings suggest that COVID-19 induces a cytokine storm in the circulation of both pregnant and non-pregnant individuals; yet, pregnant women display a dampened immune response.

The plasma proteome can discriminate COVID-19 cases from uninfected controls, even when mild or asymptomatic

Last, we evaluated the ability of the proteomic profiles to discriminate between COVID-19 cases and controls, regardless of pregnancy status. For this purpose, we developed random forests models that included up to 50 proteins and evaluated their accuracy via leave-one-out cross validation (LOOCV). The resulting proteomics model was able to accurately discriminate COVID-19 cases from controls, in the absence of any other inputs (Fig. 8a). The area under the Receiver Operating Characteristic curve (AUC) was 0.978 for the full analysis set, 0.974 for pregnant women, and 0.985 for non-pregnant individuals (Fig. 8a). The relative importance of

the proteomic predictors in the random forest model is displayed in Fig. 8b and includes several of the proteins with differential abundance as reported in Supplementary Tables 1-2. When classification models were derived separately based on disease severity, the accuracy to distinguish most severe cases (severe or critical COVID-19) from controls was higher (AUC = 0.99) than the one obtained for discriminating between controls and moderate cases (AUC = 0.94) (Fig. 8c). Of interest, similarly high accuracy was obtained also for distinguishing asymptomatic or mild cases from uninfected controls (AUC=0.95) (Fig. 8c). ISG15, MX1, ZBP1 and IFNL1 were the top four proteins most contributing to the accuracy of random forest models for discriminating all COVID-19 cases from controls, and these proteins were also among the top ones for prediction of severe and critical COVID-19 (Fig. 8d), moderate COVID-19 (Supplementary Fig. 3), and for mild or asymptomatic cases (Supplementary Fig. 4). Together, these data suggest that a shared proteomic signature can discriminate between COVID-19 patients and healthy individuals regardless of pregnancy status, and that disease severity is a driver of classification accuracy.

DISCUSSION

In this study, we utilized the SOMAScan v4.1 platform to profile over 7,000 protein targets in the peripheral blood of pregnant women and non-pregnant individuals diagnosed with COVID-19, and found that this disease drives changes in their plasma proteomes in a dose-response relation with disease severity. Importantly, we showed that the response to COVID-19 is dampened during pregnancy, regardless of disease severity. Distinct and overlapping proteomic changes were identified in pregnant and non-pregnant COVID-19 patients: pregnant women display a tailored proteomic response, potentially to protect the conceptus from the deleterious effects of inflammation, while non-pregnant women display a stronger response to fight off infection. Moreover, the stereotypical proteomic response induced by COVID-19 in the pregnant and non-pregnant state shows enrichment of mediators implicated in cytokine storm, endothelial dysfunction and angiogenesis; yet, such a response is dampened during pregnancy. Finally, we utilized machine learning to demonstrate that the plasma proteome can be used to discriminate COVID-19 patients from controls, even those who were asymptomatic or had mild symptoms.

The proteomic dysregulations after COVID-19 revealed in our current study are suggestive of a dampened systemic immune response in pregnant women compared to non-pregnant individuals, both in terms of the number of proteins affected and magnitude of changes for proteins implicated in the pregnant and non-pregnant states. This phenomenon could be secondary to physiological changes that occur during pregnancy, such as the reversible thymic involution[57-59] that impacts T-cell development[60,61], or could be a primary outcome intended to prevent aberrant immune activation that could threaten pregnancy[62,63]. Immune suppression was originally considered to be a requirement for successful pregnancy, given the immunological

puzzle of the mother displaying tolerance towards the semi-allograft fetus for 40 weeks[64]. Rather than complete inertness or unresponsiveness, as proposed by Peter Medawar[64], pregnancy has since been shown to be a state of selective immune tolerance[65-76], mediated by homeostatic cells such as regulatory T cells (Tregs)[65-70,73,74,76-86] and macrophages[81,87-95]. This concept is further supported by studies of women with autoimmune diseases such as systemic lupus erythematosus (SLE), in whom such pregnancy-specific immune adaptations can fail to occur[96,97], resulting in pregnancy complications[97,98]. Maternal peripheral blood signatures corresponding to IFN responses and immune cell subsets were shown to be significantly modulated throughout normal pregnancy, but less in pregnant SLE patients who experienced complications[97]. Moreover, pertinent to our current findings, the authors of the latter study suggested that the suppression of key immune pathways such as IFN could underlie the higher risk of severe viral infection in pregnant women[97]. Indeed, past and present viral pandemics have provided a large body of evidence showing that specific viruses, such as pandemic influenza viruses, Dengue virus, and coronaviruses, can result in disproportionately high rates of adverse outcomes in pregnant women[99]. Peripheral T and B cells show decreased numbers, greater activation-induced proliferation, and altered phenotypes during pregnancy[100,101], and such alterations can be further exacerbated by the lymphopenia that characterizes viral infections such as SARS-CoV-2[35,41,43,102]. Moreover, given the demonstrated relationship between pathological maternal T-cell activation and pregnancy complications such as preterm labor[62,63], it is imperative that maternal adaptive immunity remain under strict control until normal parturition at term[103-106].

Consistently, we recently undertook an *ex vivo* evaluation of peripheral cellular immune responses against SARS-CoV-2 particles and proteins in pregnant and non-pregnant women[30]. We demonstrated a pregnancy-specific reduction of unswitched memory-like and transitional-

like B-cell subsets[30], which is in line with a prior study showing that such reduction of B-cells is associated with COVID-19 severity[107]. Thus, given such deficiencies in peripheral adaptive immunity, pregnant women infected with SARS-CoV-2 may rely more heavily on monocytes, which are also potent contributors to anti-viral host defense[108]. Consistently, monocytes undergo substantial expansion and differentiation in patients with severe COVID-19[109-111], and we have shown that monocytes from pregnant women appear to undergo accelerated transition and activation in response to SARS-CoV-2 exposure[30], which is in line with a previous report[39]. Notably, we found that the cytokine profile of peripheral leukocytes was also impacted by pregnancy, as the release of IFN-β and IL-8 in response to SARS-CoV-2 was diminished compared to non-pregnant women[30]. The abovementioned studies, together with our current results, point to a specific dampening of the maternal proteomic response to COVID-19 to protect the fetus from heightened inflammation that could jeopardize pregnancy. This may not be the only mechanism protecting the fetus, as the placenta has also been shown to play a critical role in anti-SARS-CoV-2 defenses[35,112]. The incidence of vertical transmission of SARS-CoV-2 has been shown to be rare, which may be due in part to the minimal co-expression of the canonical viral cell entry mediators *ACE2* and *TMPRSS2* in this organ[19]. Moreover, the placenta exhibits strong anti-viral properties[113,114], and in women with COVID-19 the placental anti-viral response was shown to include the activation of leukocytes such as T cells, NK cells, and macrophages together with elevated expression of genes related to immune and cytokine signaling, even in the absence of detectable placental infection[35,112]. Thus, the diminished maternal systemic response to SARS-CoV-2 infection may be partially offset by the protective functions of the placenta, thereby preventing a cytokine storm that could damage the fetus while still ensuring a barrier to prevent viral transmission.

Herein, we found that pregnant and non-pregnant patients infected with SARS-CoV-2 exhibit a perturbed proteomic profile characterized by the enhanced release of cytokines and other mediators associated with inflammation, endothelial dysfunction, and angiogenesis. A hallmark of severe COVID-19 is the systemic inflammatory response that includes the exacerbated release of pro-inflammatory immune mediators, termed a cytokine storm[115-119]. Multiple cytokines involved in this response have been proposed as biomarkers of severity and prognosis for COVID-19[42]. Indeed, the peripheral blood concentration of cytokines, including IL-6, is highly correlated with mortality in patients with COVID-19[42,120], hinting at a key role for IL-6 in the pathophysiology of severe disease. In fact, it has been proposed that IL-6 acts as an amplifier of the inflammatory response triggered by SARS-CoV-2 by activating the NF-κB and STAT3 pathways in non-immune cells such as the vascular endothelium[121]. This concept is in line with the clinical findings showing that the cytokine storm can lead to generalized endothelial dysfunction[117,122], as was initially suspected early in the pandemic given the rapid emergence of cardiovascular complications in COVID-19 patients[123,124]. The vascular endothelium is an organ with multiple endocrine, paracrine, and autocrine functions, which are required for vascular homeostasis and regulation of vascular tone[125,126]. Therefore, any disruption in these functions can induce vasoconstriction that can progress to ischemia, inflammation, edema, and culminate in a pro-coagulant state[127]. In addition to the indirect induction of endothelial dysfunction due to the host inflammatory response[128,129], SARS-CoV-2 can also directly interact with the vascular endothelium, as evidenced by viral inclusion structures observed in vascular endothelial cells at multiple body sites in deceased COVID-19 patients[129,130]. SARS-CoV-2 binds to the ACE2 receptor to enter cells, which can impair the activity of the enzyme ACE2 to neutralize angiotensin vasopressors[122,131]. Such impaired ACE2 activity can activate the kallilkrein-

bradykinin pathway that results in increased vascular permeability[122,132]. Moreover, the activation of innate immune cells induces the release of toxic mediators such as reactive oxygen species (ROS) and vasoactive substances that can lead to inter-endothelial gaps, thereby further enhancing endothelial permeability[122]. The activation of endothelial cells leads to the production of multiple pro-coagulant factors, such as P-selectin, fibrinogen and Von Willebrand factor (VWF), which initiates the coagulation cascade[122,128]. These processes can also lead to platelet aggregation and the release of other factors such as VEGF, which upregulates the endothelial cell production of tissue factor, the primary stimulator of the coagulation cascade[122,133], ultimately leading to a pro-thrombotic state. Consistently, herein we showed that, while non-pregnant patients with COVID-19 exhibit angiogenic and inflammatory circulatory profiles, the proteome of pregnant women is characterized by a systemic inflammation without dysregulating the anti-angiogenic factor sFLT-1, which is already elevated in pregnant controls. This factor is a key mediator of the pathophysiology of preeclampsia[134,135], and is commonly utilized as a biomarker of this obstetrical syndrome[54]. Notably, initial investigations of pregnant women infected with SARS-CoV-2 had revealed the development of a preeclampsia-like syndrome[136,137]. Furthermore, later evidence supported COVID-19 as a risk factor for preeclampsia[8,138] and indicated a dose-response relationship with disease severity[7]; however, the mechanisms and causality of such an association are still poorly understood[54,138,139]. Our findings revealed that some proteins implicated in inflammatory and angiogenic processes were perturbed in patients with COVID-19, regardless of pregnancy status; yet, there were specific proteins that were only modified by SARS-CoV-2 infection in pregnancy. As preeclampsia is a primarily systemic endothelial-inflammatory obstetrical disease[54,140-144], our findings support the fact that some perturbed pathways may be shared between COVID-19 and preeclampsia. This is supported by a

previous study comparing circulating biomarkers in pregnant women with COVID-19 and those of women with preeclampsia, which demonstrated that preeclampsia and severe COVID-19 display distinct biomarker profiles[145]. Moreover, preeclampsia is a placental disease that is usually resolved after the delivery of this organ[142,146,147]; by contrast, maternal recovery from COVID-19 prior to delivery results in the disappearance of preeclampsia-like symptoms[54,136]. Yet, the similarities between these two disease states are consistent with the placental inflammatory response induced by maternal SARS-CoV-2 infection, even in asymptomatic pregnant women[35,112]. Such inflammation can affect the fetus even in the absence of vertical transmission, as we have demonstrated a mild cytokine response in the cord blood of neonates born to infected mothers[35]. Therefore, it is imperative to follow and evaluate these infants for eventual adverse outcomes, as has been suggested by recent evidence demonstrating neurodevelopmental sequelae at one year of life in children exposed to SARS-CoV-2 *in utero*[18].

The establishment of biomarkers that allow for the classification and monitoring of COVID-19 outcomes is essential to guide patient management, particularly during pregnancy. In the current study, we demonstrated that the systemic proteome can be utilized to distinguish COVID-19 patients and controls, in the absence of any other patient risk factors. Of importance, the plasma proteome was able to discriminate asymptomatic cases and those with mild symptoms from controls with high accuracy. Our findings are in line with a prior multi-omics investigation that evaluated 1,400 plasma proteins together with single-cell immune features for the classification of non-pregnant COVID-19 patients[148]. In the latter study, such integrated modeling showed value for the distinction of mild, moderate, and severe COVID-19 cases, and identified specific immune features that showed dose-response changes with disease[148]. The use of specific inflammatory mediators in the circulation to characterize COVID-19 was evaluated

since the onset of the pandemic, with elevated levels of cytokines (such as IL-6), chemokines, and interferons being reported in cases of severe COVID-19[149,150] and high systemic levels of IL-6, IL-8, and TNF at the time of hospitalization showing use as biomarkers of disease severity and mortality[42]. In-depth investigations have used longitudinal profiling of COVID-19 patients to identify multiple immune signatures that correlated with different disease trajectories[41], or utilized proteomic determinations and machine learning to identify 11 host proteins and biomarker combinations that could distinguish and predict COVID-19 outcomes[151]. Interestingly, the presence of neutralizing immunoglobulin G (IgG) autoantibodies against type I interferons has also been shown to represent a likely indicator of severe disease in COVID-19 patients, given that such autoantibodies were absent in most of the individuals with asymptomatic or mild SARS-CoV-2 infection[152]. Together with our current data, these observations point to the value of identifying specific proteomic changes that can serve as biomarkers of COVID-19 severity, particularly during the vulnerable period of pregnancy.

Collectively, the study herein represents the most comprehensive characterization of the plasma proteome of pregnant and non-pregnant individuals diagnosed with COVID-19. The findings reported herein emphasize the distinct immune modulation between the non-pregnant and pregnant states, providing insight into the pathogenesis of COVID-19 as well as a potential explanation for the more severe outcomes observed in pregnant women. Importantly, the unique proteomic profiles observed in pregnant women suggest that the preeclampsia-like syndrome in this population may differ in pathogenesis from the canonical pathways implicated in preeclampsia. Yet, further investigation is required to decipher the unique molecular mechanisms whereby SARS-CoV-2 infection induces a maternal cytokine storm and, more importantly, its effects on the offspring.

METHODS

Study design

The study involved profiling of 7,288 proteomic targets in plasma samples collected from pregnant women (n = 101) and from non-pregnant individuals (n = 93). Pregnant patients were enrolled at admission to the labor and delivery unit or at the time of attending the clinical for obstetrical indications or clinical deterioration warranting inpatient management. All patients were screened for COVID-19 according to standard clinical care. Of all controls (patients without COVID-19), those who provided samples within the same gestational age window as cases were retained. Non-pregnant patients were enrolled at time of admission for any medical indication, and all were tested for COVID-19. All analyses accounted for the age and sex of patients as well as the presence of chronic hypertension or high-risk pathology. All patients provided written informed consent, and the use of biological specimens and clinical data for research purposes was approved by the Biomedical Research Ethics Committee of the Fundacion Valle del Lili (Protocol No. 1611), Cali, Colombia. Patients diagnosed with COVID-19 were grouped as asymptomatic, mild, moderate, severe, or critically ill according to NIH classification[53].

Plasma proteomics

Maternal plasma protein abundance was determined using the SOMAmer (Slow Off-rate Modified Aptamers) platform and its reagents. This platform allows for the multiplexed quantification of 7,288 analytes corresponding to 6,596 unique protein targets[153-155]. Results herein are presented at the level of analytes, which are also interchangeably referred to as proteins. The experiments were run in batches of up to 85 samples per plate. Briefly, plasma

samples were diluted and then incubated with the respective SOMAmer mixes pre-immobilized onto streptavidin-coated beads. The beads were washed to remove all unbound proteins and other matrix constituents. Proteins that remained bound were then tagged using an NHS-biotin reagent. After the labeling reaction, the beads were exposed to an anionic competitor solution that prevents non-specific interactions from reforming after disruption. Pure cognate-SOMAmer complexes and unbound (free) SOMAmer reagents were then released from the streptavidin beads using ultraviolet light that cleaves the photo-cleavable linker used to quantitate proteins. The photo-cleavage eluate, which contains all SOMAmer reagents (some bound to a biotin-labeled protein and some free), was separated from the beads and then incubated with a second streptavidin-coated bead that binds the biotin-labeled proteins and the biotin-labeled protein-SOMAmer complexes. The free SOMAmer reagents were then removed by several washing steps. For the final elution, protein-bound SOMAmer reagents were released from their cognate proteins using denaturing conditions. These SOMAmer reagents were then quantified by hybridization to custom DNA microarrays. The Cyanine-3 signal from the SOMAmer reagent was detected on microarrays[153-155]. Proteomics profiling was performed by Somalogic, Inc. (Boulder, CO, USA).

Statistical analyses

Demographic and clinical characteristics

These data were summarized using numbers and percentages for categorical variables or medians and interquartile range (IQR) for continuous variables. Differences between cases and controls were assessed using the Fisher's exact test for categorical data and the Wilcoxon test for

508 continuous data. All statistical tests were two tailed and significance was inferred based on
509 $p<0.05$.
510
511 *Principal component analysis*
512 Protein abundances expressed as relative fluorescence units (RFU) were $\log_2$-
513 transformed to improve normality. The function *prcomp* in the R statistical language and
514 environment (www.r-project.org) was used to calculate principal components (PC). The top three
515 PC were tested for associations with COVID-19 and pregnancy status using linear models with
516 interaction terms. The dose-response relationship between a given PC and disease severity was
517 assessed using a linear model in which the response variable was the PC and the explanatory
518 variable was an ordered factor with six levels ordered in the sequence: Control, Asymptomatic,
519 Mild, Moderate, Severe, and Critical. This analysis included also pregnancy status, age, and sex
520 of participants as possible confounding variables. All statistical tests were two tailed and
521 significance was inferred based on $p<0.05$.
522
523 *Differential abundance analysis*
524 The proteomic data preprocessing, including an adaptive normalization by maximum
525 likelihood (ANML) step and a calibration step, were performed by SomaLogic, Inc. The goal of
526 these steps was to make data comparable across samples by calculating plate-specific and
527 analyte-specific scale factors. After log (base 2) transformation, data were compared between
528 pooled COVID-19 cases and controls or compared separately between each disease severity
529 group against controls. When analyzing data from pregnant women, maternal age, body mass
530 index (BMI), and linear and quadratic terms of gestational age were included as co-variates.

Analysis of data from non-pregnant subjects included adjustment for age, BMI, and sex of the participant. Models were fit using the *limma* package[156,157] in R. Protein abundance was considered to have changed significantly with COVID-19 if the fold change was >1.25 and false discovery rate (FDR)[158] adjusted p-value (q-value) was < 0.1. Spearman correlation coefficients and significance p-values were calculated to determine the similarity of $\log_2$ fold changes in protein abundance obtained for different COVID-19 severity groups against controls, both within and between pregnant and non-pregnant subjects. Proteins with opposite dysregulation due to COVID-19 between pregnant and non-pregnant groups were defined as proteins being either a) significantly changed with COVID-19 in pregnant women ($q < 0.1$, fold change > 1.25) but with opposite direction of change in non-pregnant individuals ($p < 0.05$), or b) significantly changed with COVID-19 in non-pregnant individuals ($q < 0.1$, fold change > 1.25) but with opposite direction of change in pregnant women ($p < 0.05$).

Gene ontology enrichment analysis

Proteins were mapped using the Entrez gene database[159] identifiers based on SomaLogic, Inc. protein annotation followed by Gene Ontology[160]. Biological processes over-represented among a given protein set were identified using Fisher's exact tests. Gene ontology terms with three or more hits and an adjusted enrichment q-value < 0.1 were considered as significantly enriched. The MSigDB collection [161] of curated canonical pathways (C2 collection) was also analyzed. Enrichment tests were performed using the *GOStats* package[162] in Bioconductor enrichment analyses. Biological processes over-represented among a given protein set were identified using Fisher's exact tests. Gene ontology terms with three or more hits and an adjusted enrichment q-value < 0.1 were considered as significantly enriched. The MSigDB collection [161]

554 of curated canonical pathways (C2 collection) was also analyzed. Enrichment tests were
555 performed using the *GOStats* package[162] in Bioconductor[163].
556
557 *Predictive model development*
558 To assess the value of plasma proteomic data to discriminate between COVID-19 and
559 controls, we have developed random forest models using up to 50 proteins. The proteins were
560 selected based on their importance to the accuracy of the models using the *randomForest*
561 function in R. The protein selection and random forest model fitting steps were evaluated using
562 leave-one-out cross validation (LOOCV), and receiver operating characteristic curves were
563 derived using the *pROC* package in R.
564
565 **DATA AVAILABILITY**
566 The majority of the data generated in this study are included in the manuscript and/or in
567 the Supplementary Materials.
568 Proteomic data generated in this study are available at the Gene Expression Omnibus
569 (accession number GSE207015). All software and R packages used herein are detailed in the
570 Methods.

REFERENCES

1 World Health Organization. *COVID-19 Weekly Epidemiological Update*, <https://www.who.int/emergencies/diseases/novel-coronavirus-2019/situation-reports> (2021).

2 Centers for Disease Control. *COVID-19 Data from the National Center for Health Statistics*, <https://www.cdc.gov/nchs/covid19/index.htm> (2021).

3 Lu, R. *et al.* Genomic characterisation and epidemiology of 2019 novel coronavirus: implications for virus origins and receptor binding. *Lancet* **395**, 565-574, doi:10.1016/S0140-6736(20)30251-8 (2020).

4 Zambrano, L. D. *et al.* Update: Characteristics of Symptomatic Women of Reproductive Age with Laboratory-Confirmed SARS-CoV-2 Infection by Pregnancy Status - United States, January 22-October 3, 2020. *MMWR Morb Mortal Wkly Rep* **69**, 1641-1647, doi:10.15585/mmwr.mm6944e3 (2020).

5 Jamieson, D. J. & Rasmussen, S. A. An Update on Coronavirus Disease 2019 (COVID-19) and Pregnancy. *Am J Obstet Gynecol*, doi:10.1016/j.ajog.2021.08.054 (2021).

6 Lokken, E. M. *et al.* Disease severity, pregnancy outcomes, and maternal deaths among pregnant patients with severe acute respiratory syndrome coronavirus 2 infection in Washington State. *Am J Obstet Gynecol* **225**, 77 e71-77 e14, doi:10.1016/j.ajog.2020.12.1221 (2021).

7 Lai, J. *et al.* SARS-CoV-2 and the subsequent development of preeclampsia and preterm birth: evidence of a dose-response relationship supporting causality. *Am J Obstet Gynecol*, doi:10.1016/j.ajog.2021.08.020 (2021).

8 Conde-Agudelo, A. & Romero, R. SARS-CoV-2 infection during pregnancy and risk of preeclampsia: a systematic review and meta-analysis. *Am J Obstet Gynecol* **226**, 68-89 e63, doi:10.1016/j.ajog.2021.07.009 (2022).

9 DeSisto, C. L. *et al.* Risk for Stillbirth Among Women With and Without COVID-19 at Delivery Hospitalization — United States, March 2020–September 2021. *MMWR Morb Mortal Wkly Rep* (2021).

10 Wang, Y. *et al.* Impact of Covid-19 in pregnancy on mother's psychological status and infant's neurobehavioral development: a longitudinal cohort study in China. *BMC Med* **18**, 347, doi:10.1186/s12916-020-01825-1 (2020).

11 Ayed, M. *et al.* Neurodevelopmental outcomes of infants secondary to in utero exposure to maternal SARS-CoV-2 infection: A national prospective study in Kuwait. *medRxiv*, 2021.2011.2012.21266291, doi:10.1101/2021.11.12.21266291 (2021).

12 Deoni, S. C., Beauchemin, J., Volpe, A. & V, D. S. Impact of the COVID-19 Pandemic on Early Child Cognitive Development: Initial Findings in a Longitudinal Observational Study of Child Health. *medRxiv*, doi:10.1101/2021.08.10.21261846 (2021).

13 Huang, P. *et al.* Association Between the COVID-19 Pandemic and Infant Neurodevelopment: A Comparison Before and During COVID-19. *Front Pediatr* **9**, 662165, doi:10.3389/fped.2021.662165 (2021).

14 Norman, M. *et al.* Association of Maternal SARS-CoV-2 Infection in Pregnancy With Neonatal Outcomes. *Jama* **325**, 2076-2086, doi:10.1001/jama.2021.5775 (2021).

15 Villar, J. *et al.* Maternal and Neonatal Morbidity and Mortality Among Pregnant Women With and Without COVID-19 Infection: The INTERCOVID Multinational Cohort Study. *JAMA Pediatr* **175**, 817-826, doi:10.1001/jamapediatrics.2021.1050 (2021).

16 Shook, L. L., Sullivan, E. L., Lo, J. O., Perlis, R. H. & Edlow, A. G. COVID-19 in pregnancy: implications for fetal brain development. *Trends Mol Med* **28**, 319-330, doi:10.1016/j.molmed.2022.02.004 (2022).

17 Shuffrey, L. C. *et al.* Association of Birth During the COVID-19 Pandemic With Neurodevelopmental Status at 6 Months in Infants With and Without In Utero Exposure to Maternal SARS-CoV-2 Infection. *JAMA Pediatr*, e215563, doi:10.1001/jamapediatrics.2021.5563 (2022).

18 Edlow, A. G., Castro, V. M., Shook, L. L., Kaimal, A. J. & Perlis, R. H. Neurodevelopmental Outcomes at 1 Year in Infants of Mothers Who Tested Positive for SARS-CoV-2 During Pregnancy. *JAMA Netw Open* **5**, e2215787, doi:10.1001/jamanetworkopen.2022.15787 (2022).

19 Pique-Regi, R. *et al.* Does the human placenta express the canonical cell entry mediators for SARS-CoV-2? *Elife* **9**, doi:10.7554/eLife.58716 (2020).

20 Shanes, E. D. *et al.* Placental Pathology in COVID-19. *Am J Clin Pathol* **154**, 23-32, doi:10.1093/ajcp/aqaa089 (2020).

21 Vivanti, A. J. *et al.* Transplacental transmission of SARS-CoV-2 infection. *Nat Commun* **11**, 3572, doi:10.1038/s41467-020-17436-6 (2020).

22 Zelop, C. M. & Bonney, E. A. COVID-19 in pregnancy: possible mechanisms not to be discounted. *J Matern Fetal Neonatal Med*, 1-4, doi:10.1080/14767058.2020.1807508 (2020).

23 Sharps, M. C. *et al.* A structured review of placental morphology and histopathological lesions associated with SARS-CoV-2 infection. *Placenta* **101**, 13-29, doi:10.1016/j.placenta.2020.08.018 (2020).

24 Bordt, E. A. *et al.* Maternal SARS-CoV-2 infection elicits sexually dimorphic placental immune responses. *Sci Transl Med* **13**, eabi7428, doi:10.1126/scitranslmed.abi7428 (2021).

25 Ovies, C., Semmes, E. C. & Coyne, C. B. Pregnancy influences immune responses to SARS-CoV-2. *Sci Transl Med* **13**, eabm2070, doi:10.1126/scitranslmed.abm2070 (2021).

26 Atyeo, C. *et al.* Compromised SARS-CoV-2-specific placental antibody transfer. *Cell* **184**, 628-642 e610, doi:10.1016/j.cell.2020.12.027 (2021).

27 Valdespino-Vázquez, M. Y. *et al.* Fetal and placental infection with SARS-CoV-2 in early pregnancy. *J Med Virol* **93**, 4480-4487, doi:10.1002/jmv.26965 (2021).

28 Verma, S. *et al.* SARS-CoV-2 colonization of maternal and fetal cells of the human placenta promotes alteration of local renin-angiotensin system. *Med (N Y)* **2**, 575-590.e575, doi:10.1016/j.medj.2021.04.009 (2021).

29 Shook, L. L. *et al.* SARS-CoV-2 Placentitis Associated With B.1.617.2 (Delta) Variant and Fetal Distress or Demise. *J Infect Dis* **225**, 754-758, doi:10.1093/infdis/jiac008 (2022).

30 Gomez-Lopez, N. *et al.* Distinct Cellular Immune Responses to SARS-CoV-2 in Pregnant Women. *J Immunol* **208**, 1857-1872, doi:10.4049/jimmunol.2101123 (2022).

31 Mithal, L. B. *et al.* Low-level SARS-CoV-2 viremia coincident with COVID placentitis and stillbirth. *Placenta* **121**, 79-81, doi:10.1016/j.placenta.2022.03.003 (2022).

32 Argueta, L. B. *et al.* Inflammatory responses in the placenta upon SARS-CoV-2 infection late in pregnancy. *iScience* **25**, 104223, doi:10.1016/j.isci.2022.104223 (2022).

33 Fenizia, C. *et al.* Analysis of SARS-CoV-2 vertical transmission during pregnancy. *Nat Commun* **11**, 5128, doi:10.1038/s41467-020-18933-4 (2020).

661 34 Edlow, A. G. *et al.* Assessment of Maternal and Neonatal SARS-CoV-2 Viral Load,
662 Transplacental Antibody Transfer, and Placental Pathology in Pregnancies During the
663 COVID-19 Pandemic. *JAMA Netw Open* **3**, e2030455,
664 doi:10.1001/jamanetworkopen.2020.30455 (2020).
665 35 Garcia-Flores, V. *et al.* Maternal-fetal immune responses in pregnant women infected with
666 SARS-CoV-2. *Nat Commun* **13**, 320, doi:10.1038/s41467-021-27745-z (2022).
667 36 Flannery, D. D. *et al.* Assessment of Maternal and Neonatal Cord Blood SARS-CoV-2
668 Antibodies and Placental Transfer Ratios. *JAMA Pediatr* **175**, 594-600,
669 doi:10.1001/jamapediatrics.2021.0038 (2021).
670 37 Chen, G. *et al.* Differential immune responses in pregnant patients recovered from COVID-
671 19. *Signal Transduct Target Ther* **6**, 289, doi:10.1038/s41392-021-00703-3 (2021).
672 38 Chen, G. *et al.* Immune Response to COVID-19 During Pregnancy. *Front Immunol* **12**,
673 675476, doi:10.3389/fimmu.2021.675476 (2021).
674 39 De Biasi, S. *et al.* Endogenous control of inflammation characterizes pregnant women with
675 asymptomatic or paucisymptomatic SARS-CoV-2 infection. *Nat Commun* **12**, 4677,
676 doi:10.1038/s41467-021-24940-w (2021).
677 40 Muthuka, J. K., Kiptoo, M., Oluoch, K. & Nyamai, E. An Association of Pregnancy with
678 Coronavirus Cytokine Storm: Systematic Review and Meta-Analysis. *JMIR Pediatr*
679 *Parent*, doi:10.2196/31579 (2022).
680 41 Lucas, C. *et al.* Longitudinal analyses reveal immunological misfiring in severe COVID-
681 19. *Nature* **584**, 463-469, doi:10.1038/s41586-020-2588-y (2020).
682 42 Del Valle, D. M. *et al.* An inflammatory cytokine signature predicts COVID-19 severity
683 and survival. *Nat Med* **26**, 1636-1643, doi:10.1038/s41591-020-1051-9 (2020).

43 Bernardes, J. P. *et al.* Longitudinal Multi-omics Analyses Identify Responses of Megakaryocytes, Erythroid Cells, and Plasmablasts as Hallmarks of Severe COVID-19. *Immunity* **53**, 1296-1314.e1299, doi:10.1016/j.immuni.2020.11.017 (2020).

44 Meckiff, B. J. *et al.* Imbalance of Regulatory and Cytotoxic SARS-CoV-2-Reactive CD4(+) T Cells in COVID-19. *Cell* **183**, 1340-1353 e1316, doi:10.1016/j.cell.2020.10.001 (2020).

45 Lipman, D., Safo, S. E. & Chekouo, T. Multi-omic analysis reveals enriched pathways associated with COVID-19 and COVID-19 severity. *PLoS One* **17**, e0267047, doi:10.1371/journal.pone.0267047 (2022).

46 Foo, S. S. *et al.* The systemic inflammatory landscape of COVID-19 in pregnancy: Extensive serum proteomic profiling of mother-infant dyads with in utero SARS-CoV-2. *Cell Rep Med* **2**, 100453, doi:10.1016/j.xcrm.2021.100453 (2021).

47 Romero, R. *et al.* The maternal plasma proteome changes as a function of gestational age in normal pregnancy: a longitudinal study. *Am J Obstet Gynecol* **217**, 67 e61-67 e21, doi:10.1016/j.ajog.2017.02.037 (2017).

48 Erez, O. *et al.* The prediction of late-onset preeclampsia: Results from a longitudinal proteomics study. *PLoS One* **12**, e0181468, doi:10.1371/journal.pone.0181468 (2017).

49 Tarca, A. L. *et al.* The prediction of early preeclampsia: Results from a longitudinal proteomics study. *PLoS One* **14**, e0217273, doi:10.1371/journal.pone.0217273 (2019).

50 Ghaemi, M. S. *et al.* Proteomic signatures predict preeclampsia in individual cohorts but not across cohorts - implications for clinical biomarker studies. *J Matern Fetal Neonatal Med*, 1-8, doi:10.1080/14767058.2021.1888915 (2021).

51 Tarca, A. L. *et al.* Crowdsourcing assessment of maternal blood multi-omics for predicting gestational age and preterm birth. *Cell Rep Med* **2**, 100323, doi:10.1016/j.xcrm.2021.100323 (2021).

52 Bhatti, G. *et al.* The amniotic fluid proteome changes with gestational age in normal pregnancy: a cross-sectional study. *Sci Rep* **12**, 601, doi:10.1038/s41598-021-04050-9 (2022).

53 Health, N. I. o. *Clinical Spectrum of SARS-CoV-2 Infection*, <https://www.covid19treatmentguidelines.nih.gov/overview/clinical-spectrum/> (

54 Jung, E. *et al.* The etiology of preeclampsia. *Am J Obstet Gynecol* **226**, S844-S866, doi:10.1016/j.ajog.2021.11.1356 (2022).

55 Amulic, B., Cazalet, C., Hayes, G. L., Metzler, K. D. & Zychlinsky, A. Neutrophil function: from mechanisms to disease. *Annu Rev Immunol* **30**, 459-489, doi:10.1146/annurev-immunol-020711-074942 (2012).

56 Papayannopoulos, V., Metzler, K. D., Hakkim, A. & Zychlinsky, A. Neutrophil elastase and myeloperoxidase regulate the formation of neutrophil extracellular traps. *J Cell Biol* **191**, 677-691, doi:10.1083/jcb.201006052 (2010).

57 Chambers, S. P. & Clarke, A. G. Measurement of thymus weight, lumbar node weight and progesterone levels in syngeneically pregnant, allogeneically pregnant, and pseudopregnant mice. *J Reprod Fertil* **55**, 309-315, doi:10.1530/jrf.0.0550309 (1979).

58 Shinomiya, N. *et al.* Thymic depletion in pregnancy: kinetics of thymocytes and immunologic capacities of the hosts. *J Clin Lab Immunol* **34**, 11-22 (1991).

59 Clarke, A. G. & Kendall, M. D. The thymus in pregnancy: the interplay of neural, endocrine and immune influences. *Immunol Today* **15**, 545-551, doi:10.1016/0167-5699(94)90212-7 (1994).

60 Laan, M., Haljasorg, U., Kisand, K., Salumets, A. & Peterson, P. Pregnancy-induced thymic involution is associated with suppression of chemokines essential for T-lymphoid progenitor homing. *Eur J Immunol* **46**, 2008-2017, doi:10.1002/eji.201646309 (2016).

61 Zoller, A. L., Schnell, F. J. & Kersh, G. J. Murine pregnancy leads to reduced proliferation of maternal thymocytes and decreased thymic emigration. *Immunology* **121**, 207-215, doi:10.1111/j.1365-2567.2006.02559.x (2007).

62 Gomez-Lopez, N. *et al.* In vivo T-cell activation by a monoclonal αCD3ε antibody induces preterm labor and birth. *Am J Reprod Immunol* **76**, 386-390, doi:10.1111/aji.12562 (2016).

63 Arenas-Hernandez, M. *et al.* Effector and Activated T Cells Induce Preterm Labor and Birth That Is Prevented by Treatment with Progesterone. *J Immunol* **202**, 2585-2608, doi:10.4049/jimmunol.1801350 (2019).

64 Medawar, P. B. Some immunological and endocrinological problems raised by the evolution of viviparity in vertebrates. *Symp Soc Exp Biol* **7**, 320–328 (1953).

65 Chaouat, G., Voisin, G. A., Escalier, D. & Robert, P. Facilitation reaction (enhancing antibodies and suppressor cells) and rejection reaction (sensitized cells) from the mother to the paternal antigens of the conceptus. *Clin Exp Immunol* **35**, 13-24 (1979).

66 Bonney, E. A. & Onyekwuluje, J. The H-Y response in mid-gestation and long after delivery in mice primed before pregnancy. *Immunol Invest* **32**, 71-81, doi:10.1081/imm-120019209 (2003).

67 Zenclussen, A. C. *et al.* Abnormal T-cell reactivity against paternal antigens in spontaneous abortion: adoptive transfer of pregnancy-induced CD4+CD25+ T regulatory cells prevents fetal rejection in a murine abortion model. *Am J Pathol* **166**, 811-822, doi:10.1016/s0002-9440(10)62302-4 (2005).

68 Robertson, S. A., Guerin, L. R., Moldenhauer, L. M. & Hayball, J. D. Activating T regulatory cells for tolerance in early pregnancy - the contribution of seminal fluid. *J Reprod Immunol* **83**, 109-116, doi:10.1016/j.jri.2009.08.003 (2009).

69 Kahn, D. A. & Baltimore, D. Pregnancy induces a fetal antigen-specific maternal T regulatory cell response that contributes to tolerance. *Proc Natl Acad Sci U S A* **107**, 9299-9304, doi:10.1073/pnas.1003909107 (2010).

70 Shima, T. *et al.* Regulatory T cells are necessary for implantation and maintenance of early pregnancy but not late pregnancy in allogeneic mice. *J Reprod Immunol* **85**, 121-129, doi:10.1016/j.jri.2010.02.006 (2010).

71 Zenclussen, M. L. *et al.* The persistence of paternal antigens in the maternal body is involved in regulatory T-cell expansion and fetal-maternal tolerance in murine pregnancy. *Am J Reprod Immunol* **63**, 200-208, doi:10.1111/j.1600-0897.2009.00793.x (2010).

72 Dimova, T. *et al.* Maternal Foxp3 expressing CD4+ CD25+ and CD4+ CD25- regulatory T-cell populations are enriched in human early normal pregnancy decidua: a phenotypic study of paired decidual and peripheral blood samples. *Am J Reprod Immunol* **66 Suppl 1**, 44-56, doi:10.1111/j.1600-0897.2011.01046.x (2011).

73 Rowe, J. H., Ertelt, J. M., Xin, L. & Way, S. S. Pregnancy imprints regulatory memory that sustains anergy to fetal antigen. *Nature* **490**, 102-106, doi:10.1038/nature11462 (2012).

74 Samstein, R. M., Josefowicz, S. Z., Arvey, A., Treuting, P. M. & Rudensky, A. Y. Extrathymic generation of regulatory T cells in placental mammals mitigates maternal-fetal conflict. *Cell* **150**, 29-38, doi:10.1016/j.cell.2012.05.031 (2012).

75 Ramhorst, R. *et al.* Modulation and recruitment of inducible regulatory T cells by first trimester trophoblast cells. *Am J Reprod Immunol* **67**, 17-27, doi:10.1111/j.1600-0897.2011.01056.x (2012).

76 Shima, T. *et al.* Paternal antigen-specific proliferating regulatory T cells are increased in uterine-draining lymph nodes just before implantation and in pregnant uterus just after implantation by seminal plasma-priming in allogeneic mouse pregnancy. *J Reprod Immunol* **108**, 72-82, doi:10.1016/j.jri.2015.02.005 (2015).

77 Aluvihare, V. R., Kallikourdis, M. & Betz, A. G. Regulatory T cells mediate maternal tolerance to the fetus. *Nat Immunol* **5**, 266-271, doi:10.1038/ni1037 (2004).

78 Sasaki, Y. *et al.* Decidual and peripheral blood CD4+CD25+ regulatory T cells in early pregnancy subjects and spontaneous abortion cases. *Mol Hum Reprod* **10**, 347-353, doi:10.1093/molehr/gah044 (2004).

79 Heikkinen, J., Möttönen, M., Alanen, A. & Lassila, O. Phenotypic characterization of regulatory T cells in the human decidua. *Clin Exp Immunol* **136**, 373-378, doi:10.1111/j.1365-2249.2004.02441.x (2004).

80 Jiang, T. T. *et al.* Regulatory T cells: new keys for further unlocking the enigma of fetal tolerance and pregnancy complications. *J Immunol* **192**, 4949-4956, doi:10.4049/jimmunol.1400498 (2014).

81 Svensson-Arvelund, J. *et al.* The human fetal placenta promotes tolerance against the semiallogeneic fetus by inducing regulatory T cells and homeostatic M2 macrophages. *J Immunol* **194**, 1534-1544, doi:10.4049/jimmunol.1401536 (2015).

82 Bonney, E. A. Immune Regulation in Pregnancy: A Matter of Perspective? *Obstet Gynecol Clin North Am* **43**, 679-698, doi:10.1016/j.ogc.2016.07.004 (2016).

83 Tsuda, S. *et al.* Clonally Expanded Decidual Effector Regulatory T Cells Increase in Late Gestation of Normal Pregnancy, but Not in Preeclampsia, in Humans. *Front Immunol* **9**, 1934, doi:10.3389/fimmu.2018.01934 (2018).

84 Salvany-Celades, M. *et al.* Three Types of Functional Regulatory T Cells Control T Cell Responses at the Human Maternal-Fetal Interface. *Cell Rep* **27**, 2537-2547.e2535, doi:10.1016/j.celrep.2019.04.109 (2019).

85 Gomez-Lopez, N. *et al.* Regulatory T Cells Play a Role in a Subset of Idiopathic Preterm Labor/Birth and Adverse Neonatal Outcomes. *Cell Rep* **32**, 107874, doi:10.1016/j.celrep.2020.107874 (2020).

86 Zhang, D., Lin, Y., Li, Y., Zhao, D. & Du, M. Mesenchymal stem cells enhance Treg immunosuppressive function at the fetal-maternal interface. *J Reprod Immunol* **148**, 103366, doi:10.1016/j.jri.2021.103366 (2021).

87 Hunt, J. S., Manning, L. S. & Wood, G. W. Macrophages in murine uterus are immunosuppressive. *Cell Immunol* **85**, 499-510, doi:10.1016/0008-8749(84)90262-4 (1984).

88 Gustafsson, C. *et al.* Gene expression profiling of human decidual macrophages: evidence for immunosuppressive phenotype. *PLoS One* **3**, e2078, doi:10.1371/journal.pone.0002078 (2008).

89 Nagamatsu, T. & Schust, D. J. The immunomodulatory roles of macrophages at the maternal-fetal interface. *Reprod Sci* **17**, 209-218, doi:10.1177/1933719109349962 (2010).

90 Svensson, J. *et al.* Macrophages at the fetal-maternal interface express markers of alternative activation and are induced by M-CSF and IL-10. *J Immunol* **187**, 3671-3682, doi:10.4049/jimmunol.1100130 (2011).

91 Houser, B. L., Tilburgs, T., Hill, J., Nicotra, M. L. & Strominger, J. L. Two unique human decidual macrophage populations. *J Immunol* **186**, 2633-2642, doi:10.4049/jimmunol.1003153 (2011).

92 Svensson-Arvelund, J. & Ernerudh, J. The Role of Macrophages in Promoting and Maintaining Homeostasis at the Fetal-Maternal Interface. *Am J Reprod Immunol* **74**, 100-109, doi:10.1111/aji.12357 (2015).

93 Xu, Y. *et al.* An M1-like Macrophage Polarization in Decidual Tissue during Spontaneous Preterm Labor That Is Attenuated by Rosiglitazone Treatment. *J Immunol* **196**, 2476-2491, doi:10.4049/jimmunol.1502055 (2016).

94 Chambers, M. *et al.* Macrophage Plasticity in Reproduction and Environmental Influences on Their Function. *Front Immunol* **11**, 607328, doi:10.3389/fimmu.2020.607328 (2020).

95 Gomez-Lopez, N. *et al.* Macrophages exert homeostatic actions in pregnancy to protect against preterm birth and fetal inflammatory injury. *JCI Insight* **6**, doi:10.1172/jci.insight.146089 (2021).

96 Doria, A. *et al.* Effect of pregnancy on serum cytokines in SLE patients. *Arthritis Res Ther* **14**, R66, doi:10.1186/ar3782 (2012).

97 Hong, S. *et al.* Longitudinal profiling of human blood transcriptome in healthy and lupus pregnancy. *J Exp Med* **216**, 1154-1169, doi:10.1084/jem.20190185 (2019).

98 Bundhun, P. K., Soogund, M. Z. & Huang, F. Impact of systemic lupus erythematosus on maternal and fetal outcomes following pregnancy: A meta-analysis of studies published between years 2001-2016. *J Autoimmun* **79**, 17-27, doi:10.1016/j.jaut.2017.02.009 (2017).

99 Cornish, E. F., Filipovic, I., Asenius, F., Williams, D. J. & McDonnell, T. Innate Immune Responses to Acute Viral Infection During Pregnancy. *Front Immunol* **11**, 572567, doi:10.3389/fimmu.2020.572567 (2020).

100 Kraus, T. A. *et al.* Characterizing the pregnancy immune phenotype: results of the viral immunity and pregnancy (VIP) study. *J Clin Immunol* **32**, 300-311, doi:10.1007/s10875-011-9627-2 (2012).

101 Demery-Poulos, C. *et al.* Pregnancy imparts distinct systemic adaptive immune function. *Am J Reprod Immunol* (Submitted, 2022).

102 Song, J. W. *et al.* Immunological and inflammatory profiles in mild and severe cases of COVID-19. *Nat Commun* **11**, 3410, doi:10.1038/s41467-020-17240-2 (2020).

103 Aghaeepour, N. *et al.* An immune clock of human pregnancy. *Sci Immunol* **2**, doi:10.1126/sciimmunol.aan2946 (2017).

104 Gomez-Lopez, N. *et al.* The Cellular Transcriptome in the Maternal Circulation During Normal Pregnancy: A Longitudinal Study. *Front Immunol* **10**, 2863, doi:10.3389/fimmu.2019.02863 (2019).

105 Han, X. *et al.* Differential Dynamics of the Maternal Immune System in Healthy Pregnancy and Preeclampsia. *Front Immunol* **10**, 1305, doi:10.3389/fimmu.2019.01305 (2019).

106 Tarca, A. L. *et al.* Targeted expression profiling by RNA-Seq improves detection of cellular dynamics during pregnancy and identifies a role for T cells in term parturition. *Sci Rep* **9**, 848, doi:10.1038/s41598-018-36649-w (2019).

107 Sosa-Hernandez, V. A. *et al.* B Cell Subsets as Severity-Associated Signatures in COVID-19 Patients. *Front Immunol* **11**, 611004, doi:10.3389/fimmu.2020.611004 (2020).

108 Nikitina, E., Larionova, I., Choinzonov, E. & Kzhyshkowska, J. Monocytes and Macrophages as Viral Targets and Reservoirs. *Int J Mol Sci* **19**, doi:10.3390/ijms19092821 (2018).

109 Wen, W. *et al.* Immune cell profiling of COVID-19 patients in the recovery stage by single-cell sequencing. *Cell Discov* **6**, 31, doi:10.1038/s41421-020-0168-9 (2020).

110 Chilunda, V. *et al.* Transcriptional Changes in CD16+ Monocytes May Contribute to the Pathogenesis of COVID-19. *Front Immunol* **12**, 665773, doi:10.3389/fimmu.2021.665773 (2021).

111 Zhang, D. *et al.* Frontline Science: COVID-19 infection induces readily detectable morphologic and inflammation-related phenotypic changes in peripheral blood monocytes. *J Leukoc Biol* **109**, 13-22, doi:10.1002/jlb.4hi0720-470r (2021).

112 Lu-Culligan, A. *et al.* Maternal respiratory SARS-CoV-2 infection in pregnancy is associated with a robust inflammatory response at the maternal-fetal interface. *Med (N Y)* **2**, 591-610 e510, doi:10.1016/j.medj.2021.04.016 (2021).

113 Delorme-Axford, E., Sadovsky, Y. & Coyne, C. B. The Placenta as a Barrier to Viral Infections. *Annu Rev Virol* **1**, 133-146, doi:10.1146/annurev-virology-031413-085524 (2014).

114 Megli, C. J. & Coyne, C. B. Infections at the maternal-fetal interface: an overview of pathogenesis and defence. *Nat Rev Microbiol* **20**, 67-82, doi:10.1038/s41579-021-00610-y (2022).

883 115 Mehta, P. *et al.* COVID-19: consider cytokine storm syndromes and immunosuppression.
884 *Lancet* **395**, 1033-1034, doi:10.1016/s0140-6736(20)30628-0 (2020).
885 116 Moore, J. B. & June, C. H. Cytokine release syndrome in severe COVID-19. *Science* **368**,
886 473-474, doi:10.1126/science.abb8925 (2020).
887 117 Pedersen, S. F. & Ho, Y. C. SARS-CoV-2: a storm is raging. *J Clin Invest* **130**, 2202-2205,
888 doi:10.1172/jci137647 (2020).
889 118 Tay, M. Z., Poh, C. M., Rénia, L., MacAry, P. A. & Ng, L. F. P. The trinity of COVID-19:
890 immunity, inflammation and intervention. *Nat Rev Immunol* **20**, 363-374,
891 doi:10.1038/s41577-020-0311-8 (2020).
892 119 Hu, B., Huang, S. & Yin, L. The cytokine storm and COVID-19. *J Med Virol* **93**, 250-256,
893 doi:10.1002/jmv.26232 (2021).
894 120 Santa Cruz, A. *et al.* Interleukin-6 Is a Biomarker for the Development of Fatal Severe
895 Acute Respiratory Syndrome Coronavirus 2 Pneumonia. *Front Immunol* **12**, 613422,
896 doi:10.3389/fimmu.2021.613422 (2021).
897 121 Hojyo, S. *et al.* How COVID-19 induces cytokine storm with high mortality. *Inflamm*
898 *Regen* **40**, 37, doi:10.1186/s41232-020-00146-3 (2020).
899 122 Teuwen, L. A., Geldhof, V., Pasut, A. & Carmeliet, P. COVID-19: the vasculature
900 unleashed. *Nat Rev Immunol* **20**, 389-391, doi:10.1038/s41577-020-0343-0 (2020).
901 123 Guo, T. *et al.* Cardiovascular Implications of Fatal Outcomes of Patients With Coronavirus
902 Disease 2019 (COVID-19). *JAMA Cardiol* **5**, 811-818, doi:10.1001/jamacardio.2020.1017
903 (2020).
904 124 Zheng, Y. Y., Ma, Y. T., Zhang, J. Y. & Xie, X. COVID-19 and the cardiovascular system.
905 *Nat Rev Cardiol* **17**, 259-260, doi:10.1038/s41569-020-0360-5 (2020).

125 Vane, J. R., Anggard, E. E. & Botting, R. M. Regulatory functions of the vascular endothelium. *N Engl J Med* **323**, 27-36, doi:10.1056/NEJM199007053230106 (1990).

126 Flammer, A. J. *et al.* The assessment of endothelial function: from research into clinical practice. *Circulation* **126**, 753-767, doi:10.1161/CIRCULATIONAHA.112.093245 (2012).

127 Celermajer, D. S. Endothelial dysfunction: does it matter? Is it reversible? *J Am Coll Cardiol* **30**, 325-333, doi:10.1016/s0735-1097(97)00189-7 (1997).

128 Evans, P. C. *et al.* Endothelial dysfunction in COVID-19: a position paper of the ESC Working Group for Atherosclerosis and Vascular Biology, and the ESC Council of Basic Cardiovascular Science. *Cardiovasc Res* **116**, 2177-2184, doi:10.1093/cvr/cvaa230 (2020).

129 Varga, Z. *et al.* Endothelial cell infection and endotheliitis in COVID-19. *Lancet* **395**, 1417-1418, doi:10.1016/S0140-6736(20)30937-5 (2020).

130 Ackermann, M. *et al.* Pulmonary Vascular Endothelialitis, Thrombosis, and Angiogenesis in Covid-19. *N Engl J Med* **383**, 120-128, doi:10.1056/NEJMoa2015432 (2020).

131 Hoffmann, M. *et al.* SARS-CoV-2 Cell Entry Depends on ACE2 and TMPRSS2 and Is Blocked by a Clinically Proven Protease Inhibitor. *Cell* **181**, 271-280 e278, doi:10.1016/j.cell.2020.02.052 (2020).

132 Nagashima, S. *et al.* COVID-19 and Lung Mast Cells: The Kallikrein-Kinin Activation Pathway. *Int J Mol Sci* **23**, doi:10.3390/ijms23031714 (2022).

133 Giesen, P. L. *et al.* Blood-borne tissue factor: another view of thrombosis. *Proc Natl Acad Sci U S A* **96**, 2311-2315, doi:10.1073/pnas.96.5.2311 (1999).

134 Maynard, S. E. *et al.* Excess placental soluble fms-like tyrosine kinase 1 (sFlt1) may contribute to endothelial dysfunction, hypertension, and proteinuria in preeclampsia. *J Clin Invest* **111**, 649-658, doi:10.1172/JCI17189 (2003).

135 Luttun, A. & Carmeliet, P. Soluble VEGF receptor Flt1: the elusive preeclampsia factor discovered? *J Clin Invest* **111**, 600-602, doi:10.1172/JCI18015 (2003).

136 Mendoza, M. *et al.* Pre-eclampsia-like syndrome induced by severe COVID-19: a prospective observational study. *BJOG* **127**, 1374-1380, doi:10.1111/1471-0528.16339 (2020).

137 Rosenbloom, J. I., Raghuraman, N., Carter, E. B. & Kelly, J. C. Coronavirus disease 2019 infection and hypertensive disorders of pregnancy. *Am J Obstet Gynecol* **224**, 623-624, doi:10.1016/j.ajog.2021.03.001 (2021).

138 Khalil, A., Samara, A., Chowdhury, T. & O'Brien, P. Does COVID-19 cause pre-eclampsia? *Ultrasound Obstet Gynecol* **59**, 146-152, doi:10.1002/uog.24809 (2022).

139 Conde-Agudelo, A. & Romero, R. Mechanisms that may underlie a causal association between SARS-COV-2 infection and preeclampsia. *Am J Obstet Gynecol* **226**, 280-281, doi:10.1016/j.ajog.2021.09.007 (2022).

140 Redman, C. W. Immunological aspects of pre-eclampsia. *Baillieres Clin Obstet Gynaecol* **6**, 601-615, doi:10.1016/s0950-3552(05)80012-4 (1992).

141 Borzychowski, A. M., Sargent, I. L. & Redman, C. W. Inflammation and pre-eclampsia. *Semin Fetal Neonatal Med* **11**, 309-316, doi:10.1016/j.siny.2006.04.001 (2006).

142 Erez, O. *et al.* Preeclampsia and eclampsia: the conceptual evolution of a syndrome. *Am J Obstet Gynecol* **226**, S786-s803, doi:10.1016/j.ajog.2021.12.001 (2022).

143 Miller, D. *et al.* Cellular immune responses in the pathophysiology of preeclampsia. *J Leukoc Biol* **111**, 237-260, doi:10.1002/jlb.5ru1120-787rr (2022).

144 Staff, A. C. *et al.* Failure of physiological transformation and spiral artery atherosis: their roles in preeclampsia. *Am J Obstet Gynecol* **226**, S895-s906, doi:10.1016/j.ajog.2020.09.026 (2022).

145 Palomo, M. *et al.* Differences and similarities in endothelial and angiogenic profiles of preeclampsia and COVID-19 in pregnancy. *Am J Obstet Gynecol*, doi:10.1016/j.ajog.2022.03.048 (2022).

146 Chaiworapongsa, T., Chaemsaithong, P., Yeo, L. & Romero, R. Pre-eclampsia part 1: current understanding of its pathophysiology. *Nat Rev Nephrol* **10**, 466-480, doi:10.1038/nrneph.2014.102 (2014).

147 Hauspurg, A. & Jeyabalan, A. Postpartum preeclampsia or eclampsia: defining its place and management among the hypertensive disorders of pregnancy. *Am J Obstet Gynecol* **226**, S1211-s1221, doi:10.1016/j.ajog.2020.10.027 (2022).

148 Feyaerts, D. *et al.* Integrated plasma proteomic and single-cell immune signaling network signatures demarcate mild, moderate, and severe COVID-19. *bioRxiv*, doi:10.1101/2021.02.09.430269 (2021).

149 Blanco-Melo, D. *et al.* Imbalanced Host Response to SARS-CoV-2 Drives Development of COVID-19. *Cell* **181**, 1036-1045.e1039, doi:10.1016/j.cell.2020.04.026 (2020).

150 Laing, A. G. *et al.* A dynamic COVID-19 immune signature includes associations with poor prognosis. *Nat Med* **26**, 1623-1635, doi:10.1038/s41591-020-1038-6 (2020).

151 Shu, T. *et al.* Plasma Proteomics Identify Biomarkers and Pathogenesis of COVID-19. *Immunity* **53**, 1108-1122 e1105, doi:10.1016/j.immuni.2020.10.008 (2020).

152 Bastard, P. *et al.* Autoantibodies against type I IFNs in patients with life-threatening COVID-19. *Science* **370**, doi:10.1126/science.abd4585 (2020).

153 Gold, L. *et al.* Aptamer-based multiplexed proteomic technology for biomarker discovery. *PLoS One* **5**, e15004, doi:10.1371/journal.pone.0015004 (2010).

154 Davies, D. R. *et al.* Unique motifs and hydrophobic interactions shape the binding of modified DNA ligands to protein targets. *Proc Natl Acad Sci U S A* **109**, 19971-19976, doi:10.1073/pnas.1213933109 (2012).

155 SomaLogic. *SOMAmer Technical notes: http://www.somalogic.com/somalogic/media/Assets/PDFs/SSM-017-Rev-3-SOMAmer-Technical-Note-3-7-15.pdf*.

156 Smyth, G. K. in *Bioinformatics and Computational Biology Solutions Using R and Bioconductor* (eds R. Gentleman *et al.*) 397-420 (Springer, 2012).

157 Ritchie, M. E. *et al.* limma powers differential expression analyses for RNA-sequencing and microarray studies. *Nucleic Acids Res* **43**, e47, doi:10.1093/nar/gkv007 (2015).

158 Benjamini, Y. & Hochberg, Y. Controlling the false discovery rate: a practical and powerful approach to multiple testing. *J Royal Stat Soc B* **57**, 289-300 (1995).

159 Maglott, D., Ostell, J., Pruitt, K. D. & Tatusova, T. Entrez Gene: gene-centered information at NCBI. *Nucleic Acids Res* **33**, D54-58, doi:10.1093/nar/gki031 (2005).

160 Ashburner, M. *et al.* Gene ontology: tool for the unification of biology. The Gene Ontology Consortium. *Nat Genet* **25**, 25-29, doi:10.1038/75556 (2000).

161 Liberzon, A. *et al.* The Molecular Signatures Database (MSigDB) hallmark gene set collection. *Cell Syst* **1**, 417-425, doi:10.1016/j.cels.2015.12.004 (2015).

162 Falcon, S. & Gentleman, R. Using GOstats to test gene lists for GO term association. *Bioinformatics* **23**, 257-258, doi:10.1093/bioinformatics/btl567 (2007).

163 Gentleman, R. C. *et al.* Bioconductor: open software development for computational biology and bioinformatics. *Genome Biol* **5**, R80, doi:10.1186/gb-2004-5-10-r80 (2004).

ACKNOWLEDGEMENTS

This research was supported by the Perinatology Research Branch, Division of Obstetrics and Maternal-Fetal Medicine, Division of Intramural Research, *Eunice Kennedy Shriver* National Institute of Child Health and Human Development, National Institutes of Health, U.S. Department of Health and Human Services (NICHD/NIH/DHHS) under Contract No. HHSN275201300006C (R.R.). This research was also supported by the Wayne State University Perinatal Initiative in Maternal, Perinatal and Child Health (N.G-L. and A.L.T.) and the Clinical Research Center, Department of Pathology and Laboratory Medicine, High Obstetric Complexity Unit, and Intensive Care Unit of the Fundacion Valle del Lili (M.F.E). R.R. has contributed to this work as part of his official duties as an employee of the United States Federal Government.

AUTHOR CONTRIBUTIONS

NG-L: designed and supervised the study, analyzed data, provided intellectual input, and wrote the paper. RR: conceived and designed the study, analyzed data, provided intellectual input, and wrote the paper. MFE: conceived, designed and supervised the study, analyzed data, and provided intellectual input. JAC, MPE, and LLA: DN: provided human samples used in the study, analyzed and recorded data. DM: analyzed data, provided intellectual input, and wrote the paper. DMG: analyze data and provided intellectual input. JG and MA-H: analyzed data, provided intellectual input, and wrote the paper. GB and BD: analyzed data and provided intellectual input. MAZ, IR, PAF, and LP: provided human samples used in the study and recorded data. TC, EJ, VG-F, MS, FG, MB, and NGT: provided intellectual input. ALT: designed and supervised the study, analyzed data, provided intellectual input, and wrote the paper.

DECLARATION OF INTERESTS

The authors declare no competing interests.

MATERIALS AND CORRESPONDENCE

Correspondence and requests for materials should be addressed to N.G-L. and A.L.T.

FIGURE LEGENDS

Fig. 1. The plasma proteome of COVID-19 patients differs according to disease severity and pregnancy status. (a) Illustration of the study design showing the number of non-pregnant controls (n = 41; 22 male, 19 female), non-pregnant COVID-19 cases (n = 52; 22 male, 30 female) pregnant controls (n = 29), and pregnant COVID-19 cases (n = 72) from whom peripheral plasma samples were profiled. **(b)** Gestational age at sampling (grey circle) and at delivery (green triangle) for each pregnant control (upper panel) and case (lower panel). **(c)** UMAP representation of the plasma proteome of pregnant controls and cases. Black = control, grey = asymptomatic case, blue = mild case, yellow = moderate case, red = severe case, brown = critical case. **(d)** Principal component (PC) plot of the plasma proteome of all study samples according to PC1 and PC2. Black = control, red = case. Circle = non-pregnant, triangle = pregnant. Increasing shape size corresponds to increasing COVID-19 severity. **(e)** PC plot representing the relationship between the plasma proteome of all study samples according to PC1 and PC3. **(f)** Violin plot representing the relationship between PC3 and COVID-19 severity among all study samples.

Fig. 2. The plasma proteome shows increasing perturbation with COVID-19 severity in pregnancy. (a) Graphical representation showing the comparison of plasma proteomes between each classified subset of pregnant COVID-19 cases and controls. **(b)** Volcano plot showing the proteins modulated in asymptomatic COVID-19 cases compared to controls. Red = proteins with $q < 0.1$ and fold change > 1.25, green = proteins with $q \geq 0.1$ and fold change > 1.25, grey = proteins with $q \geq 0.1$ and fold change ≤ 1.25, blue = proteins with $q < 0.1$ and fold change ≤ 1.25. **(c)** Volcano plot showing the proteins modulated in mild COVID-19 cases compared to controls.

(d) Volcano plot showing the proteins modulated in moderate COVID-19 cases compared to controls. **(e)** Volcano plot showing the proteins modulated in severe COVID-19 cases compared to controls. **(f)** Volcano plot showing the proteins modulated in critical COVID-19 cases compared to controls. **(g)** Comparison of the magnitude in proteomic changes among pregnant COVID-19 case subsets, using the comparison between critical cases vs. controls as the reference. Spearman's correlation and p-value are provided for the asymptomatic vs. control, mild vs. control, moderate vs. control, and severe vs. control contrasts compared to the reference. The proteins included in this analysis (grey dots) are those 1,072 identified as differentially abundant in the comparison between pregnant critically ill cases vs. controls.

Fig. 3. The plasma proteome shows increasing perturbation with COVID-19 severity in non-pregnant individuals. (a) Graphical representation showing the comparison of plasma proteomes between each classified subset of non-pregnant COVID-19 cases and controls. **(b)** Volcano plot showing the proteins modulated in moderate COVID-19 cases compared to controls. Red = proteins with $q < 0.1$ and fold change > 1.25, green = proteins with $q \geq 0.1$ and fold change > 1.25, grey = proteins with $q \geq 0.1$ and fold change ≤ 1.25, blue = proteins with $q < 0.1$ and fold change ≤ 1.25. **(c)** Volcano plot showing the proteins modulated in severe COVID-19 cases compared to controls. **(d)** Volcano plot showing the proteins modulated in critical COVID-19 cases compared to controls. **(e)** Comparison of the magnitude in proteomic changes among non-pregnant COVID-19 case subsets, using the comparison between critical cases vs. controls as the reference. Spearman's correlation and p-value are provided for the moderate vs. control and severe vs. control contrasts compared to the reference. The proteins included in this

analysis (grey dots) are those 2,966 identified as differentially abundant in the comparison between non-pregnant critically ill cases vs. controls.

Fig. 4. The protein response to COVID-19 is dampened in pregnancy regardless of disease severity. (a) Graphical representation showing the comparison of 486 plasma proteins that are modulated in both pregnant COVID-19 cases vs. controls and in non-pregnant COVID-19 cases vs. controls. **(b)** Correlation between the magnitude of proteomic changes in pregnant moderate cases vs. controls and that in non-pregnant moderate cases vs. controls. Slope of the regression line (red line), Spearman's correlation, and p-value are provided. Dotted blue line represents the parity line. **(c)** Correlation between the magnitude of proteomic changes in pregnant severe cases vs. controls and that in non-pregnant severe cases vs. controls. **(d)** Correlation between the magnitude of proteomic changes in pregnant critical cases vs. controls and that in non-pregnant critical cases vs. controls.

Fig. 5. The biological processes and pathways perturbed after COVID-19 differ between pregnant and non-pregnant patients. (a) Volcano plot showing the proteins modulated in all pregnant COVID-19 cases compared to controls. Red = proteins with $q < 0.1$ and fold change > 1.25, green = proteins with $q \geq 0.1$ and fold change > 1.25, grey = proteins with $q \geq 0.1$ and fold change ≤ 1.25, blue = proteins with $q < 0.1$ and fold change ≤ 1.25. **(b)** Volcano plot showing the proteins modulated in all non-pregnant COVID-19 cases compared to controls. **(c)** Venn diagram showing the overlap of biological processes enriched among proteins modulated by COVID-19 between pregnant and non-pregnant cases compared to controls. **(d)** Bar plot showing the odds ratios for top biological processes enriched among proteins modulated by COVID-19 in pregnant

cases compared to controls. Asterisk indicates odds ratio calculated as "infinite". **(e)** Bar plot showing the odds ratios for top biological processes enriched among proteins modulated by COVID-19 in non-pregnant cases compared to controls. **(f)** Bar plot showing the odds ratios for top biological processes enriched among proteins modulated by COVID-19 in both pregnant and non-pregnant cases compared to controls. **(g)** Venn diagram showing the overlap of C2 pathways enriched among proteins modulated by COVID-19 in pregnant and non-pregnant cases compared to controls. **(h)** Bar plot showing the odds ratios for top C2 pathways enriched among proteins modulated by COVID-19 in pregnant cases compared to controls. **(i)** Bar plot showing the odds ratios for top C2 pathways enriched among proteins modulated by COVID-19 in non-pregnant cases compared to controls. **(j)** Bar plot showing the odds ratios for top C2 pathways enriched among proteins modulated by COVID-19 in both pregnant and non-pregnant cases compared to controls.

Fig. 6. COVID-19 drives distinct angiogenic and inflammatory profiles in pregnant and non-pregnant individuals. (a) (Left) Representative diagram illustrating the comparison between pregnant and non-pregnant COVID-19 cases and controls for specific proteins associated with angiogenesis, endothelial dysfunction, and intravascular inflammation. **(Right)** A core set of 33 proteins that are significantly modulated with COVID-19 in opposite directions between pregnant and non-pregnant patients. Note the negative slope and correlation coefficient. **(b-g)** Violin plots showing the modulation of **(b)** sFLT-1, **(c)** AGT, **(d)** TNFRSF1B, **(e)** VWF, **(f)** ELANE, and **(g)** H3C1 levels with COVID-19 severity in non-pregnant and pregnant cases and controls. Black = control, grey = asymptomatic, blue = mild, yellow = moderate, red = severe, brown = critical. RFU = relative fluorescence units.

Fig. 7. Pregnant women with COVID-19 display a dampened systemic cytokine response. **(a)** Representative diagram illustrating the evaluation and comparison of specific cytokines in the circulation of pregnant and non-pregnant COVID-19 cases and controls. **(b-n)** Violin plots showing the modulation of **(b)** IL-6, **(c)** IL-1β, **(d)** IL-18, **(e)** TNF, **(f)** IL-17A, **(g)** IL-1α, **(h)** IFNγ, **(i)** IL-10, **(j)** TGFβ1, **(k)** CCL1, **(l)** CCL22, **(m)** CXCL13, and **(n)** CXCL10 levels with COVID-19 severity in non-pregnant and pregnant cases and controls. Black = control, grey = asymptomatic, blue = mild, yellow = moderate, red = severe, brown = critical. RFU = relative fluorescence units.

Fig. 8. The plasma proteome allows for identification of COVID-19 patients and can distinguish mild and severe disease. (a) Receiver operating characteristic (ROC) curves for discrimination of all COVID-19 cases (black curve), only pregnant COVID-19 cases (red curve), and only non-pregnant COVID-19 cases (blue curve) from respective control groups. Area-under-the-curve (AUC) values are shown for each curve. **(b)** Bar plot displaying the relative importance of the top 50 proteomic predictors for identifying all COVID-19 cases. **(c)** ROC curves for discrimination of severe/critical cases from controls (red curve), moderate cases from controls (yellow curve), and asymptomatic/mild cases from controls (blue curve). **(d)** Bar plot displaying the relative importance of the top 50 proteomic predictors for distinguishing severe/critical COVID-19 cases from controls.

TABLES

Table 1. Patient demographics.

Pregnant	Controls (n = 29)	Cases (n = 72)	p-value
Age (years)	29 (25-33)	29 (25-33.2)	0.75
BMI	30.8 (27.2-37.3)	30.3 (27-32.9)	0.27
Nulliparous	75.9% (22/29)	56.9% (41/72)	0.11
Chronic hypertension	13.8% (4/29)	5.6% (4/72)	0.22
Gestational age at sampling (weeks)	36.1 (32.6-37.5)	31.3 (28.1-35.6)	0.003
Gestational age at delivery (weeks)	37.2 (34.6-38)	37.1 (34.9-38.3)	1.00
Preeclampsia	31% (9/29)	18.1% (13/72)	0.19
Non-pregnant	**Controls (n = 41)**	**Cases (n = 52)**	**p-value**
Age (years)	55 (40-63)	59.5 (42.8-69.2)	0.09
BMI	25.9 (24.1-28.4)	27.1 (25-30.8)	0.14
Male	53.7% (22/41)	42.3% (22/52)	0.30
Chronic hypertension	43.9% (18/41)	51.9% (27/52)	0.53

Data are presented as medians with interquartile ranges or as proportions (n/N).
*Missing one datum
**Missing 12 data

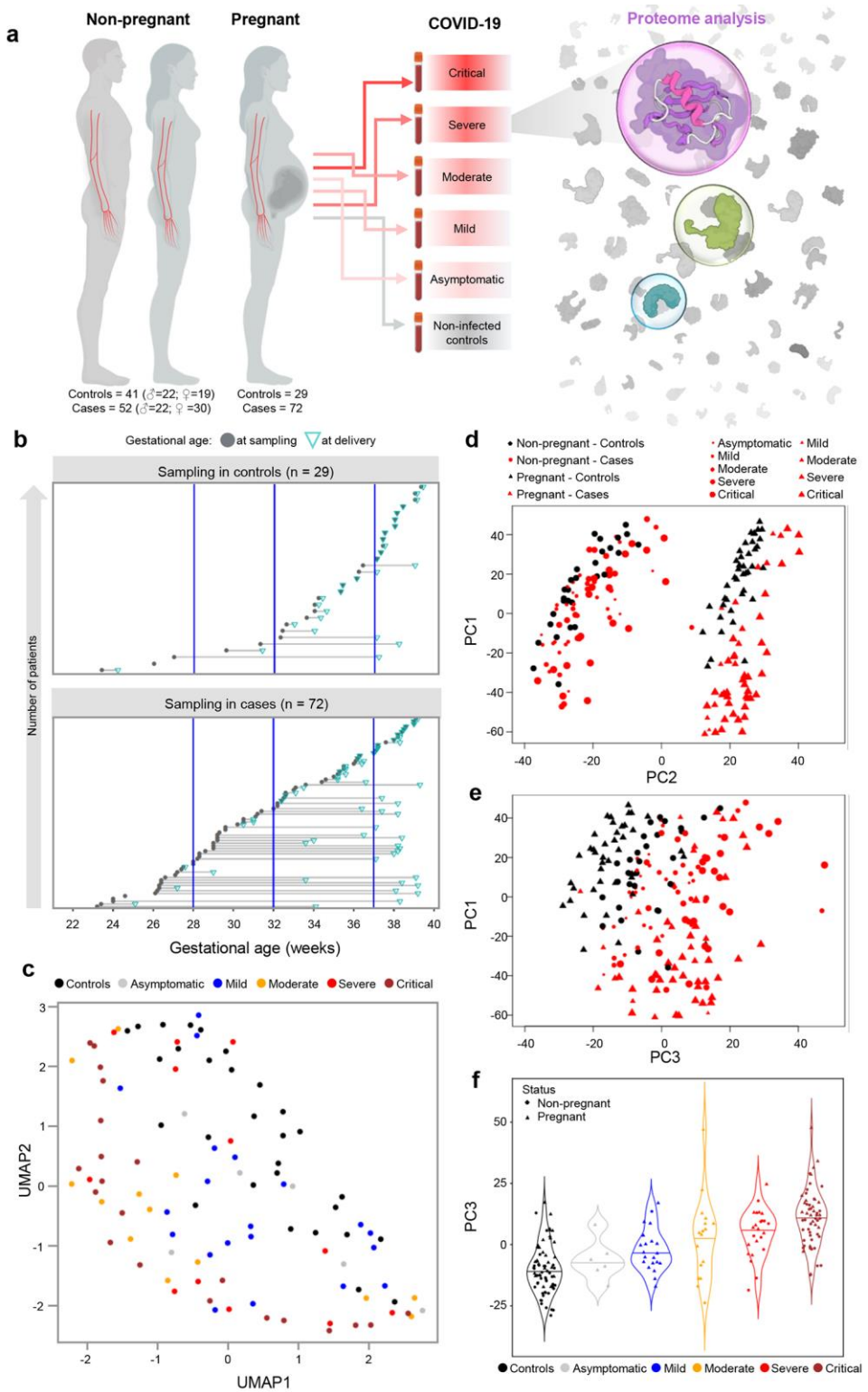

Fig. 1. The plasma proteome of COVID-19 patients differs according to disease severity and pregnancy status. (a) Illustration of the study design showing the number of non-pregnant controls (n = 41; 22 male, 19 female), non-pregnant COVID-19 cases (n = 52; 22 male, 30 female) pregnant controls (n = 29), and pregnant COVID-19 cases (n = 72) from whom peripheral plasma samples were profiled. **(b)** Gestational age at sampling (grey circle) and at delivery (green triangle) for each pregnant control (upper panel) and case (lower panel). **(c)** UMAP representation of the plasma proteome of pregnant controls and cases. Black = control, grey = asymptomatic case, blue = mild case, yellow = moderate case, red = severe case, brown = critical case. **(d)** Principal component (PC) plot of the plasma proteome of all study samples according to PC1 and PC2. Black = control, red = case. Circle = non-pregnant, triangle = pregnant. Increasing shape size corresponds to increasing COVID-19 severity. **(e)** PC plot representing the relationship between the plasma proteome of all study samples according to PC1 and PC3. **(f)** Violin plot representing the relationship between PC3 and COVID-19 severity among all study samples.

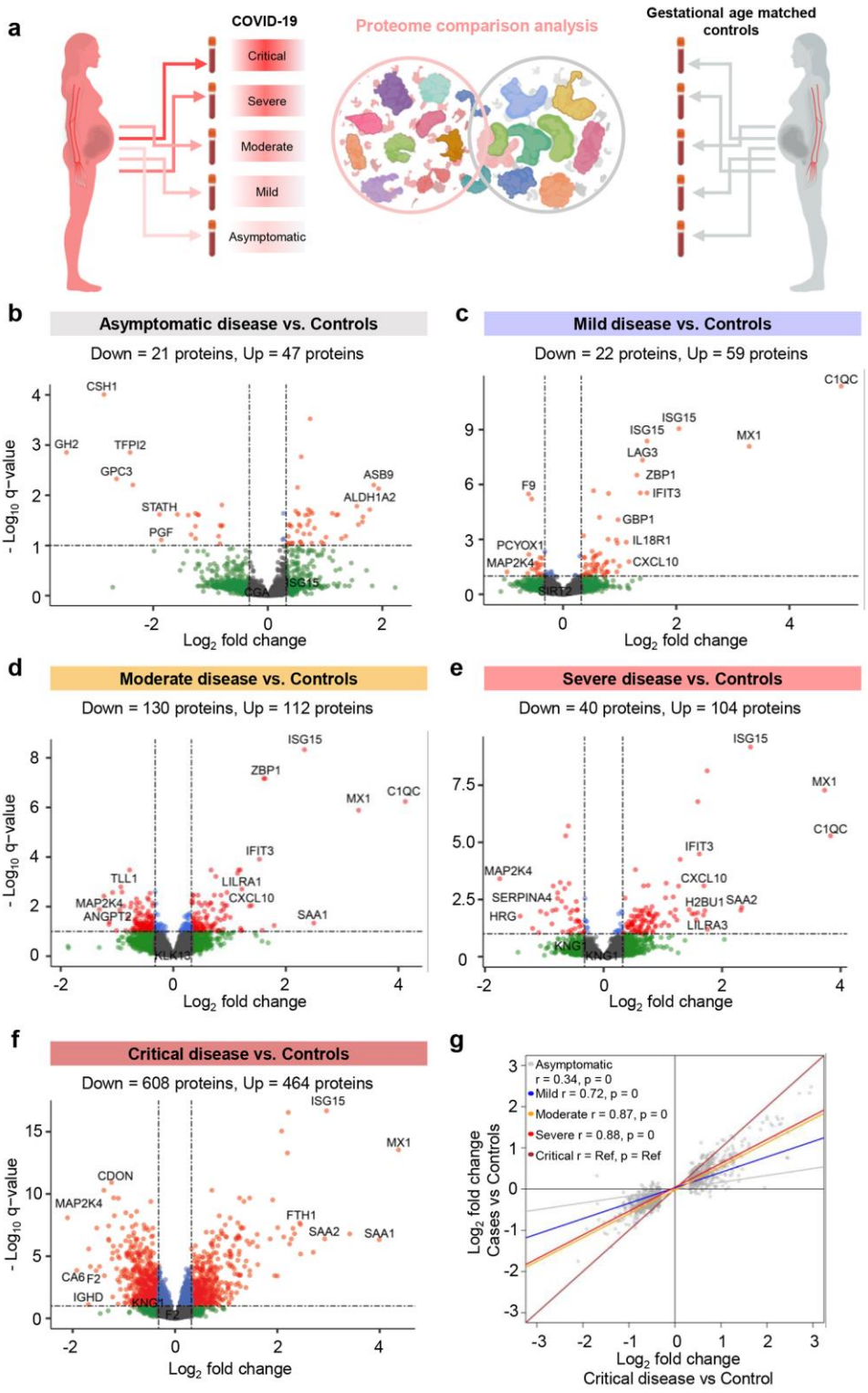

Fig. 2. The plasma proteome shows increasing perturbation with COVID-19 severity in pregnancy. **(a)** Graphical representation showing the comparison of plasma proteomes between each classified subset of pregnant COVID-19 cases and controls. **(b)** Volcano plot showing the proteins modulated in asymptomatic COVID-19 cases compared to controls. Red = proteins with q < 0.1 and fold change > 1.25, green = proteins with q ≥ 0.1 and fold change > 1.25, grey = proteins with q ≥ 0.1 and fold change ≤ 1.25, blue = proteins with q <0.1 and fold change ≤ 1.25. **(c)** Volcano plot showing the proteins modulated in mild COVID-19 cases compared to controls. **(d)** Volcano plot showing the proteins modulated in moderate COVID-19 cases compared to controls. **(e)** Volcano plot showing the proteins modulated in severe COVID-19 cases compared to controls. **(f)** Volcano plot showing the proteins modulated in critical COVID-19 cases compared to controls. **(g)** Comparison of the magnitude in proteomic changes among pregnant COVID-19 case subsets, using the comparison between critical cases vs. controls as the reference. Spearman's correlation and p-value are provided for the asymptomatic vs. control, mild vs. control, moderate vs. control, and severe vs. control contrasts compared to the reference. The proteins included in this analysis (grey dots) are those 1,072 identified as differentially abundant in the comparison between pregnant critically ill cases vs. controls.

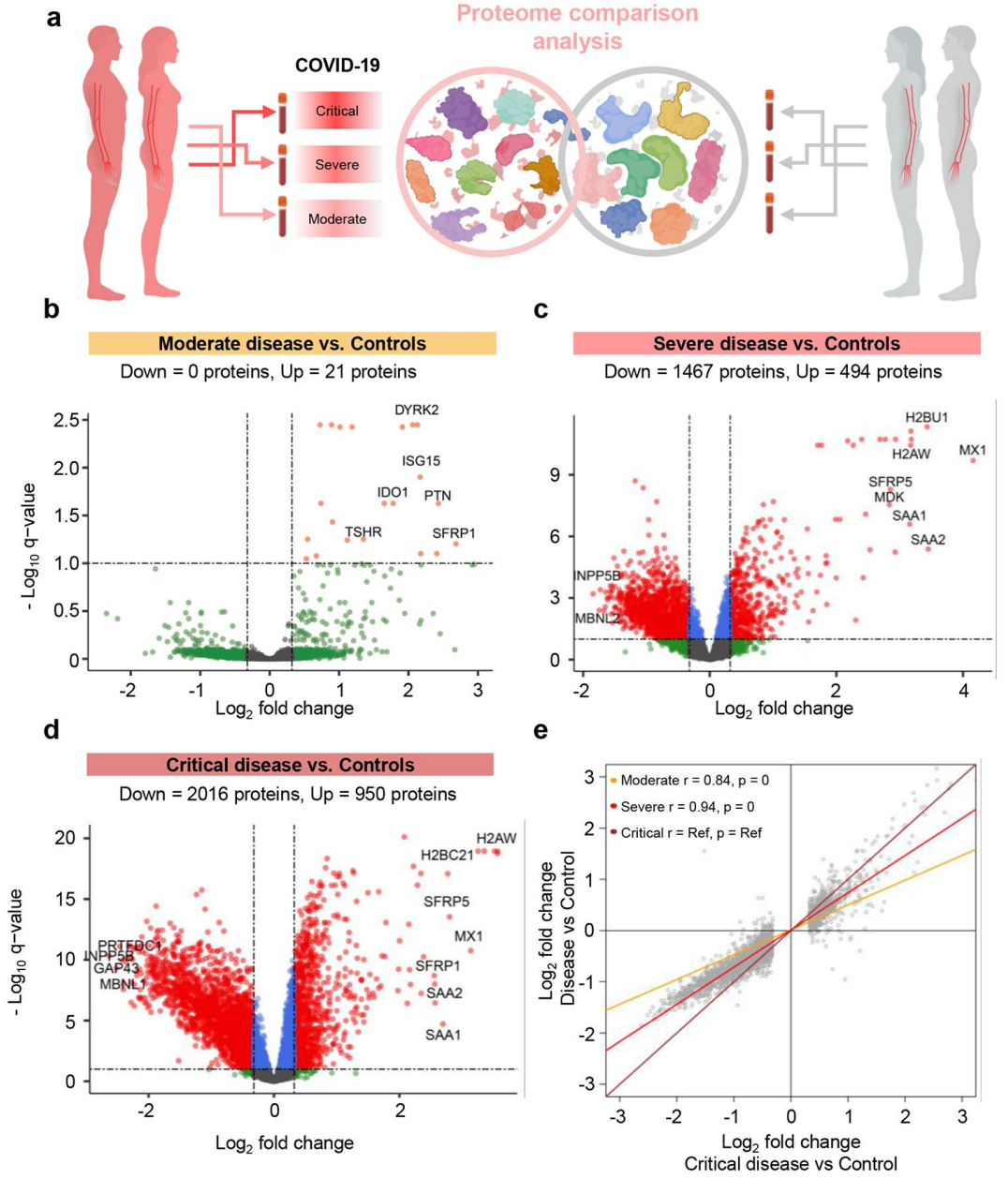

Fig. 3. The plasma proteome shows increasing perturbation with COVID-19 severity in non-pregnant individuals. (a) Graphical representation showing the comparison of plasma proteomes between each classified subset of non-pregnant COVID-19 cases and controls. **(b)** Volcano plot showing the proteins modulated in moderate COVID-19 cases compared to controls. Red = proteins with $q < 0.1$ and fold change > 1.25, green = proteins with $q \geq 0.1$ and fold change > 1.25, grey = proteins with $q \geq 0.1$ and fold change ≤ 1.25, blue = proteins with $q < 0.1$ and fold change ≤ 1.25. **(c)** Volcano plot showing the proteins modulated in severe COVID-19 cases compared to controls. **(d)** Volcano plot showing the proteins modulated in critical COVID-19 cases compared to controls. **(e)** Comparison of the magnitude in proteomic changes among non-pregnant COVID-19 case subsets, using the comparison between critical cases vs. controls as the reference. Spearman's correlation and p-value are provided for the moderate vs. control and severe vs. control contrasts compared to the reference. The proteins included in this analysis (grey dots) are those 2,966 identified as differentially abundant in the comparison between non-pregnant critically ill cases vs. controls.

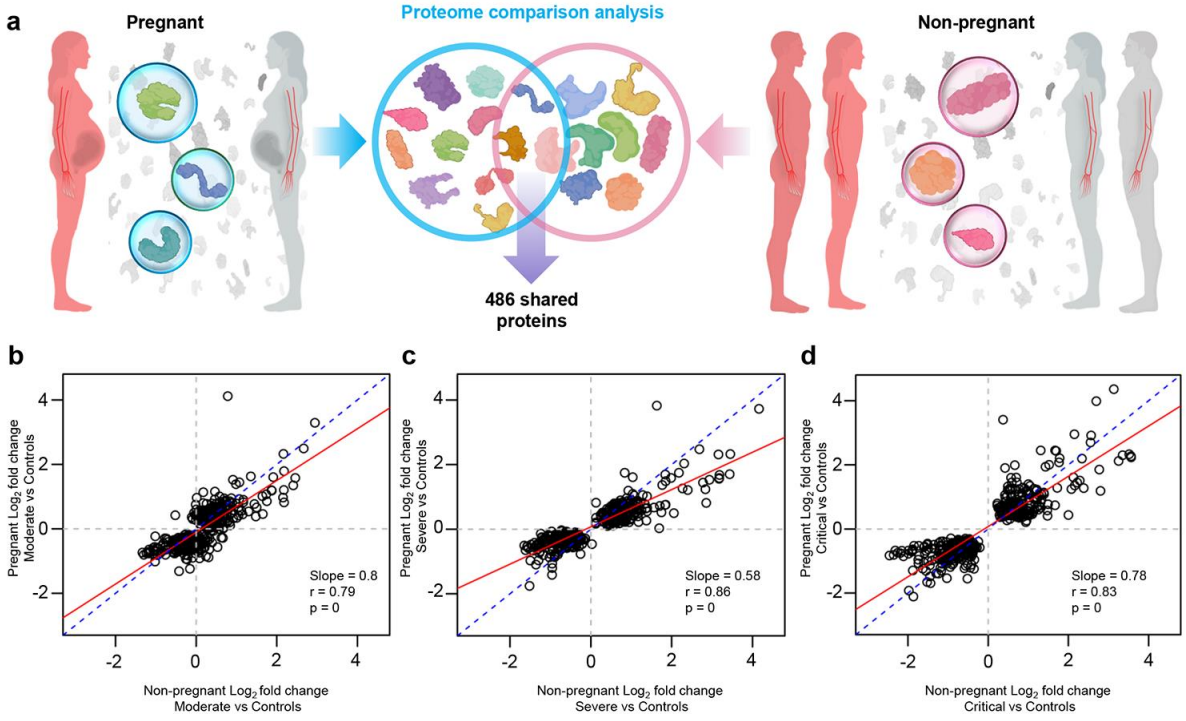

Fig. 4. The protein response to COVID-19 is dampened in pregnancy regardless of disease severity. (a) Graphical representation showing the comparison of 486 plasma proteins that are modulated in both pregnant COVID-19 cases vs. controls and in non-pregnant COVID-19 cases vs. controls. **(b)** Correlation between the magnitude of proteomic changes in pregnant moderate cases vs. controls and that in non-pregnant moderate cases vs. controls. Slope of the regression line (red line), Spearman's correlation, and p-value are provided. Dotted blue line represents the parity line. **(c)** Correlation between the magnitude of proteomic changes in pregnant severe cases vs. controls and that in non-pregnant severe cases vs. controls. **(d)** Correlation between the magnitude of proteomic changes in pregnant critical cases vs. controls and that in non-pregnant critical cases vs. controls.

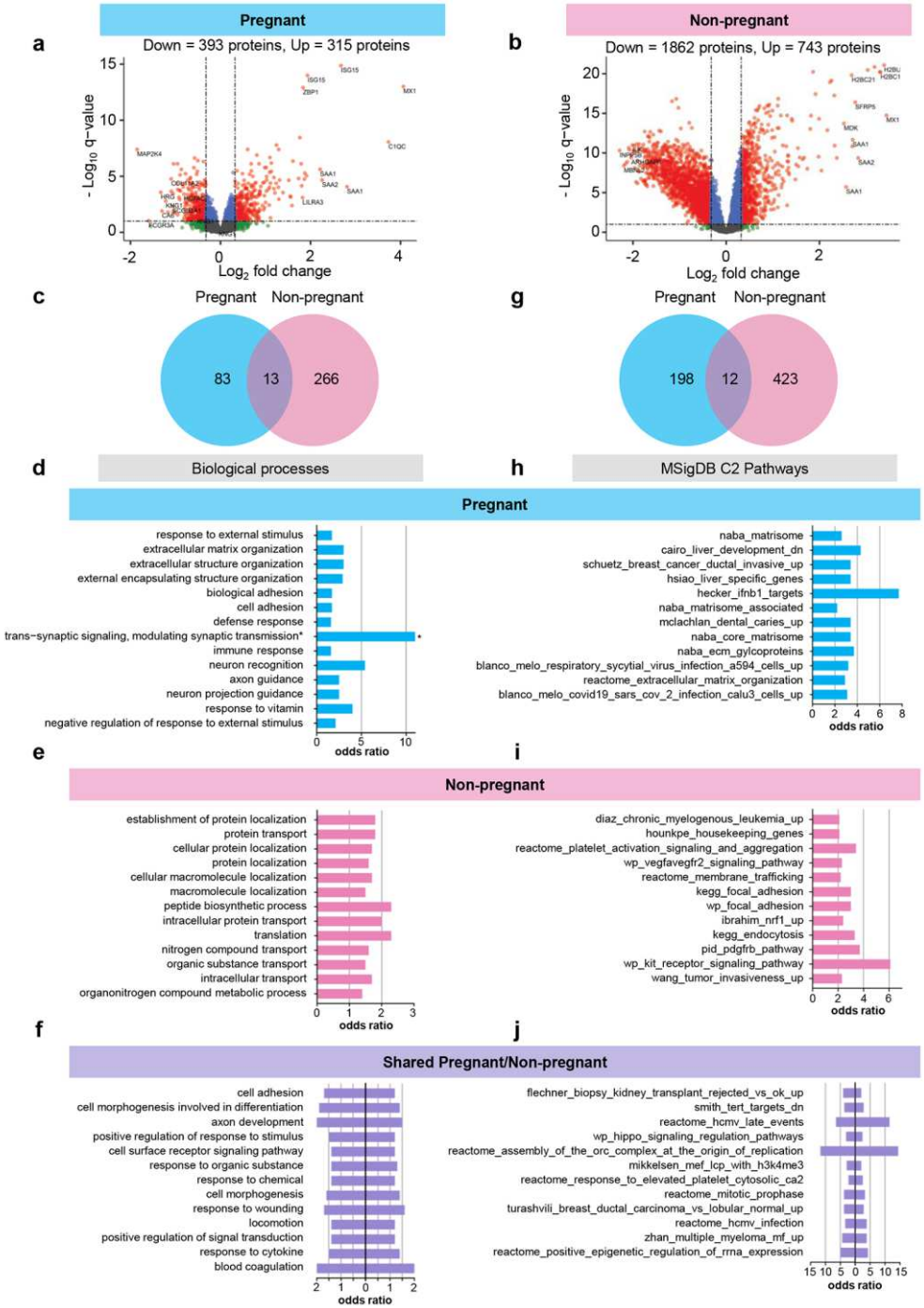

Fig. 5. The biological processes and pathways perturbed after COVID-19 differ between pregnant and non-pregnant patients. **(a)** Volcano plot showing the proteins modulated in all pregnant COVID-19 cases compared to controls. Red = proteins with $q < 0.1$ and fold change > 1.25, green = proteins with $q \geq 0.1$ and fold change > 1.25, grey = proteins with $q \geq 0.1$ and fold change ≤ 1.25, blue = proteins with $q < 0.1$ and fold change ≤ 1.25. **(b)** Volcano plot showing the proteins modulated in all non-pregnant COVID-19 cases compared to controls. **(c)** Venn diagram showing the overlap of biological processes enriched among proteins modulated by COVID-19 between pregnant and non-pregnant cases compared to controls. **(d)** Bar plot showing the odds ratios for top biological processes enriched among proteins modulated by COVID-19 in pregnant cases compared to controls. Asterisk indicates odds ratio calculated as "infinite". **(e)** Bar plot showing the odds ratios for top biological processes enriched among proteins modulated by COVID-19 in non-pregnant cases compared to controls. **(f)** Bar plot showing the odds ratios for top biological processes enriched among proteins modulated by COVID-19 in both pregnant and non-pregnant cases compared to controls. **(g)** Venn diagram showing the overlap of C2 pathways enriched among proteins modulated by COVID-19 in pregnant and non-pregnant cases compared to controls. **(h)** Bar plot showing the odds ratios for top C2 pathways enriched among proteins modulated by COVID-19 in pregnant cases compared to controls. **(i)** Bar plot showing the odds ratios for top C2 pathways enriched among proteins modulated by COVID-19 in non-pregnant cases compared to controls. **(j)** Bar plot showing the odds ratios for top C2 pathways enriched among proteins modulated by COVID-19 in both pregnant and non-pregnant cases compared to controls.

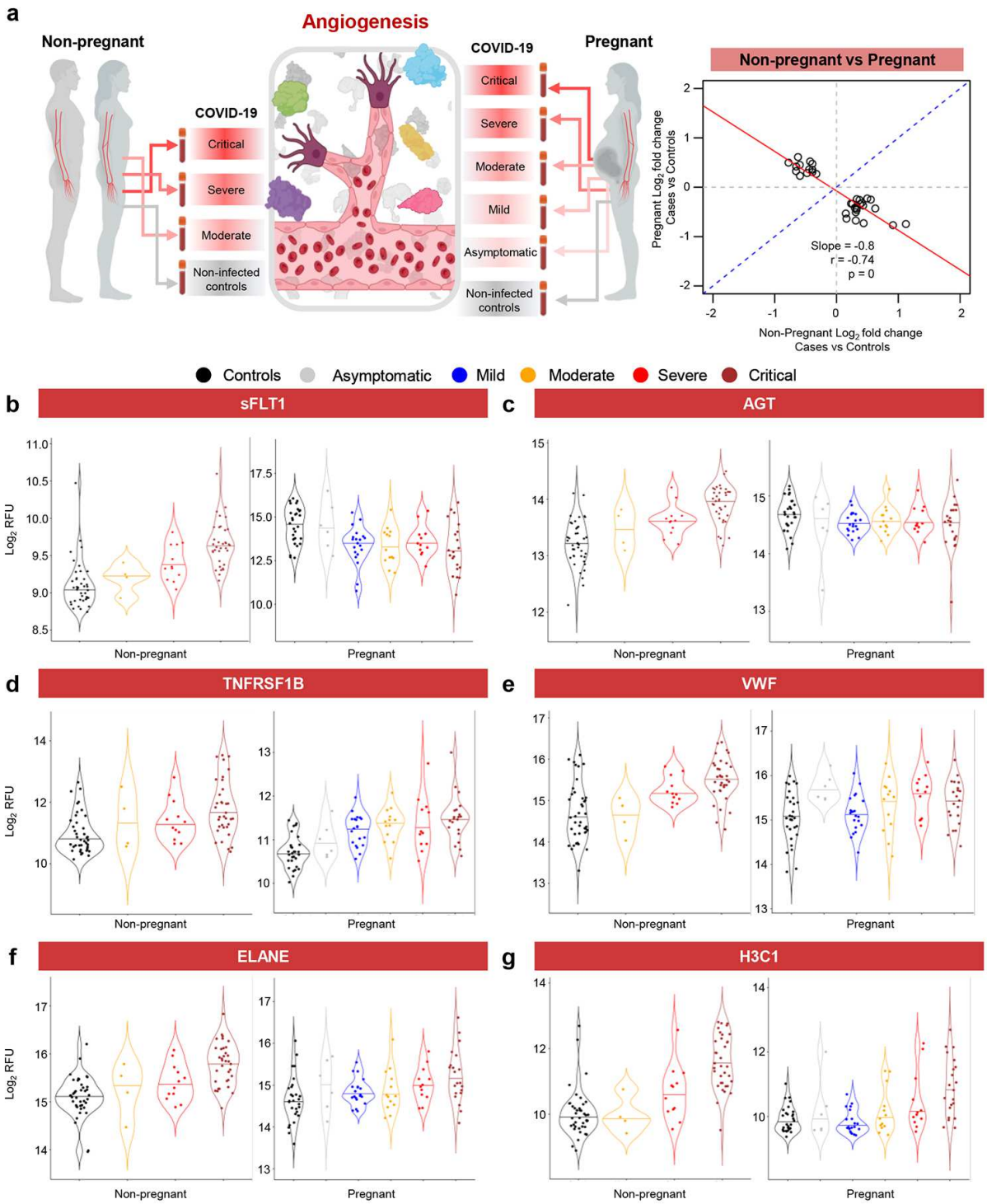

Fig. 6. COVID-19 drives distinct angiogenic and inflammatory profiles in pregnant and non-pregnant individuals. (a) (Left) Representative diagram illustrating the comparison between pregnant and non-pregnant COVID-19 cases and controls for specific proteins associated with angiogenesis, endothelial dysfunction, and intravascular inflammation. **(Right)** A core set of 33 proteins that are significantly modulated with COVID-19 in opposite directions between pregnant and non-pregnant patients. Note the negative slope and correlation coefficient. **(b-g)** Violin plots showing the modulation of **(b)** sFLT-1, **(c)** AGT, **(d)** TNFRSF1B, **(e)** VWF, **(f)** ELANE, and **(g)** H3C1 levels with COVID-19 severity in non-pregnant and pregnant cases and controls. Black = control, grey = asymptomatic, blue = mild, yellow = moderate, red = severe, brown = critical. RFU = relative fluorescence units.

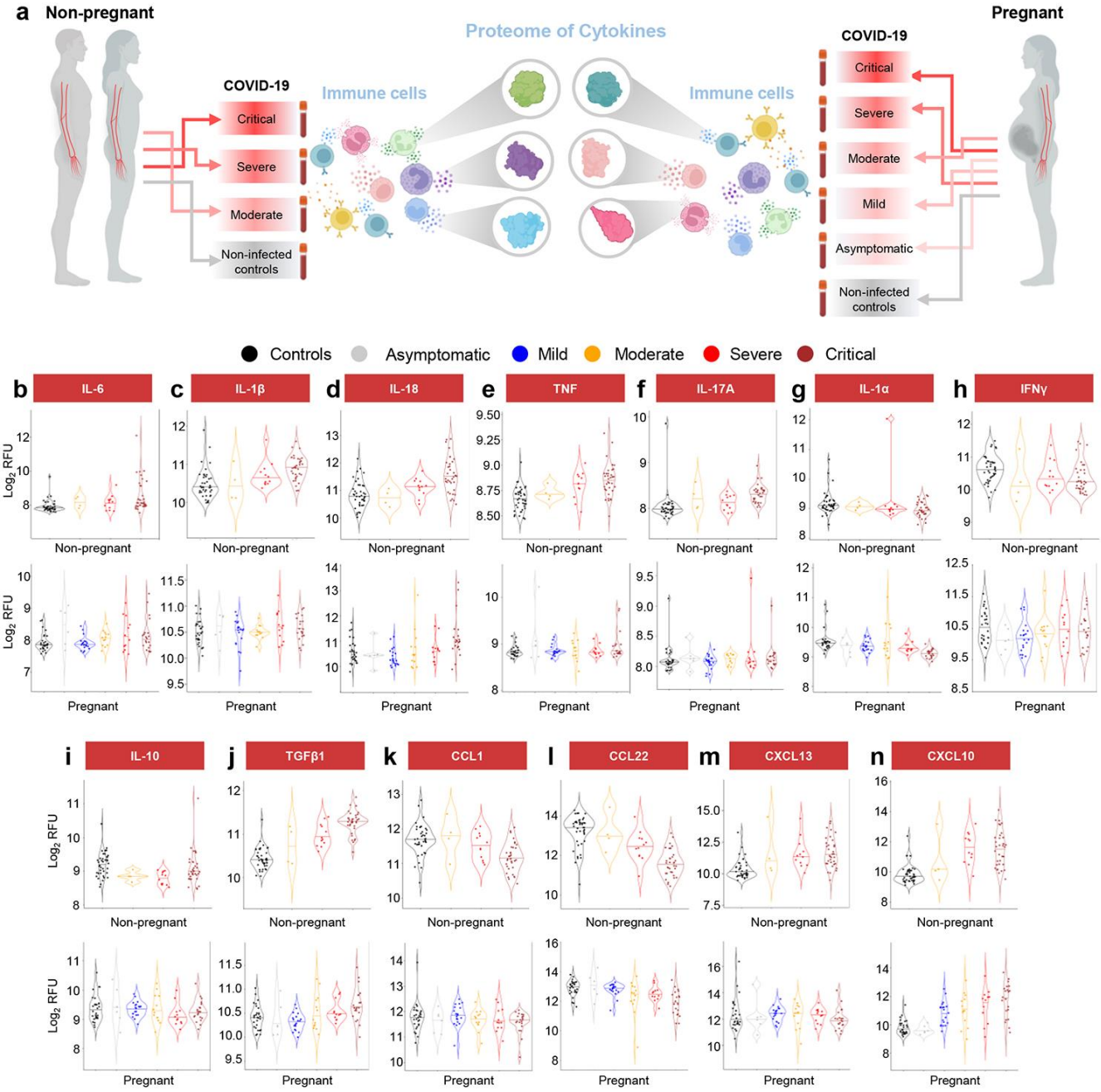

Fig. 7. Pregnant women with COVID-19 display a dampened systemic cytokine response. **(a)** Representative diagram illustrating the evaluation and comparison of specific cytokines in the circulation of pregnant and non-pregnant COVID-19 cases and controls. **(b-n)** Violin plots showing the modulation of **(b)** IL-6, **(c)** IL-1β, **(d)** IL-18, **(e)** TNF, **(f)** IL-17A, **(g)** IL-1α, **(h)** IFNγ, **(i)** IL-10, **(j)** TGFβ1, **(k)** CCL1, **(l)** CCL22, **(m)** CXCL13, and **(n)** CXCL10 levels with COVID-19 severity in non-pregnant and pregnant cases and controls. Black = control, grey = asymptomatic, blue = mild, yellow = moderate, red = severe, brown = critical. RFU = relative fluorescence units.

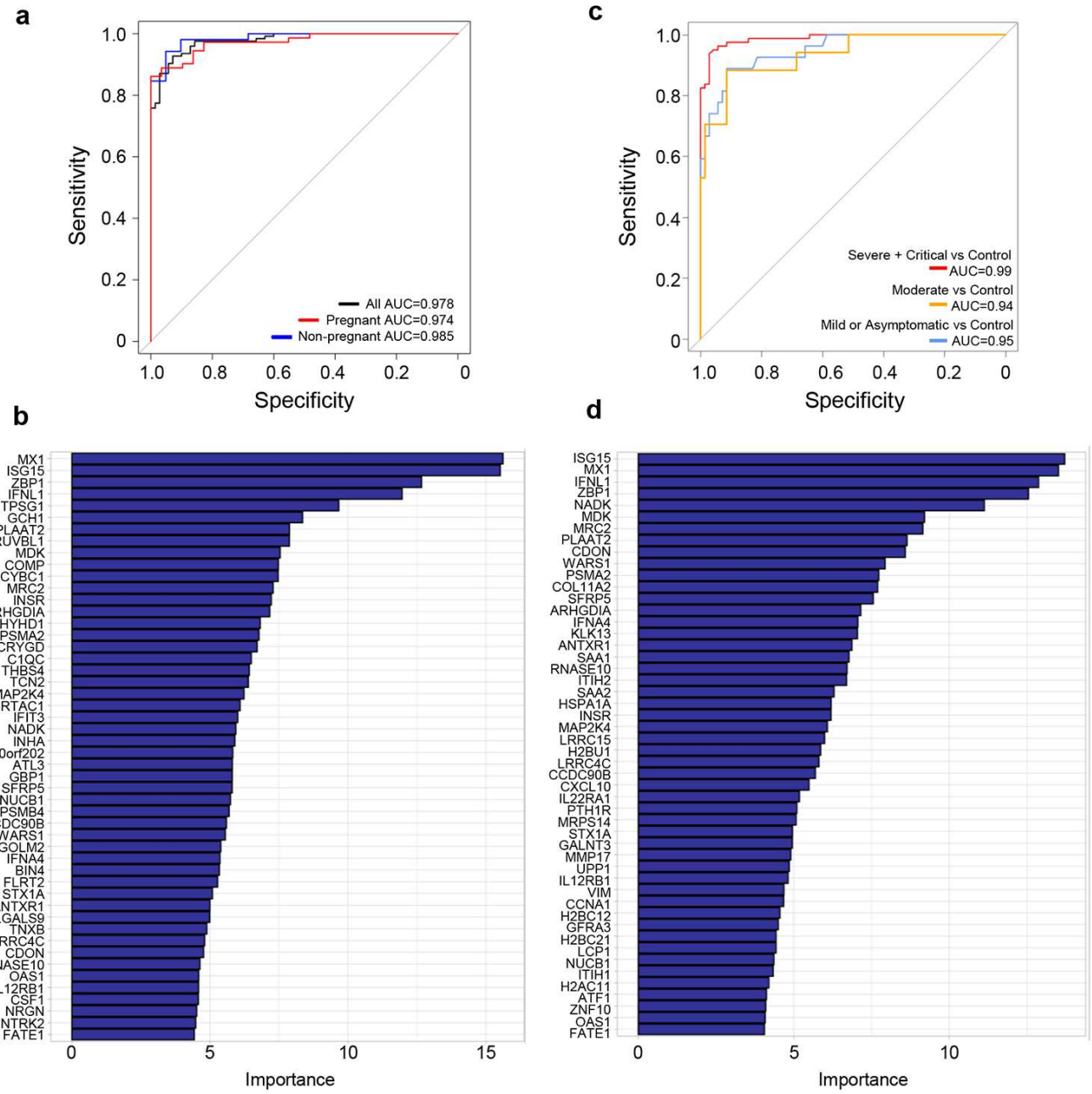

Fig. 8. The plasma proteome allows for identification of COVID-19 patients and can distinguish mild and severe disease. **(a)** Receiver operating characteristic (ROC) curves for discrimination of all COVID-19 cases (black curve), only pregnant COVID-19 cases (red curve), and only non-pregnant COVID-19 cases (blue curve) from respective control groups. Area-under-the-curve (AUC) values are shown for each curve. **(b)** Bar plot displaying the relative importance of the top 50 proteomic predictors for identifying all COVID-19 cases. **(c)** ROC curves for discrimination of severe/critical cases from controls (red curve), moderate cases from controls (yellow curve), and asymptomatic/mild cases from controls (blue curve). **(d)** Bar plot displaying the relative importance of the top 50 proteomic predictors for distinguishing severe/critical COVID-19 cases from controls.

Supplementary Files

This is a list of supplementary files associated with this preprint. Click to download.

- Table2oppositesignproteinstrendpnew.xlsx
- TableS1TotalProteinsPregnantCOVID19.xlsx
- TableS2totalProteinsNonPregnantCOVID19new.xlsx
- TableS3BPinPregResponseCOVID19.xlsx
- TableS4BPinNonPregResponseCOVID19.xlsx
- TableS5C2inPregResponseCOVID19.xlsx
- TableS6C2inNonPregResponseCOVID19.xlsx
- TableS7OffsignCasesControlsBPandC2.xlsx
- SupplementaryFigures.pdf